

First-Time Disclosure of CVN424, a Potent and Selective GPR6 Inverse Agonist for the Treatment of Parkinson's Disease: Discovery, Pharmacological Validation, and Identification of a Clinical Candidate

Huikai Sun,* Holger Monenschein,* Hans H. Schiffer, Holly A. Reichard, Shota Kikuchi, Maria Hopkins, Todd K. Macklin, Stephen Hitchcock, Mark Adams, Jason Green, Jason Brown, Sean T. Murphy, Nidhi Kaushal, Deanna R. Colia, Steve Moore, William J. Ray, Mark Beresford Lewis Carlton, and Nicola L. Brice

Cite This: <https://doi.org/10.1021/acs.jmedchem.0c02081>

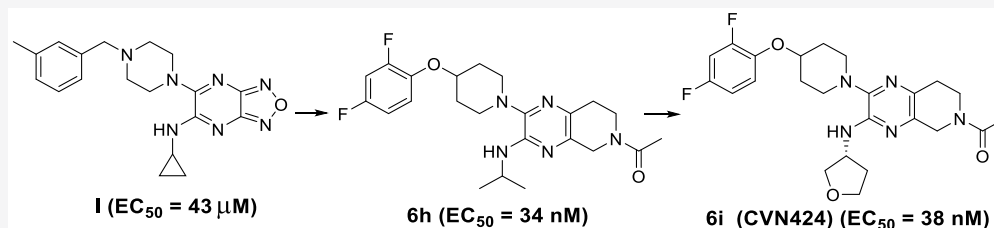
Read Online

ACCESS |

Metrics & More

Article Recommendations

Supporting Information



ABSTRACT: Parkinson's disease (PD) is a chronic and progressive movement disorder with the urgent unmet need for efficient symptomatic therapies with fewer side effects. GPR6 is an orphan G-protein coupled receptor (GPCR) with highly restricted expression in dopamine receptor D2-type medium spiny neurons (MSNs) of the indirect pathway, a striatal brain circuit which shows aberrant hyperactivity in PD patients. Potent and selective GPR6 inverse agonists (IAG) were developed starting from a low-potency screening hit ($EC_{50} = 43 \mu M$). Herein, we describe the multiple parameter optimization that led to the discovery of multiple nanomolar potent and selective GPR6 IAG, including our clinical compound CVN424. GPR6 IAG reversed haloperidol-induced catalepsy in rats and restored mobility in the bilateral 6-OHDA-lesioned rat PD model demonstrating that inhibition of GPR6 activity *in vivo* normalizes activity in basal ganglia circuitry and motor behavior. CVN424 is currently in clinical development to treat motor symptoms in Parkinson's disease.

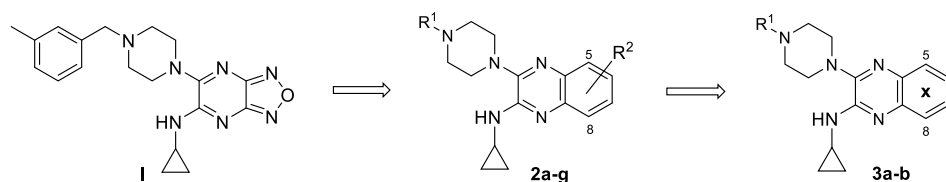
INTRODUCTION AND BIOLOGICAL RATIONALE

Parkinson's disease (PD) is a chronic and progressive movement disorder.^{1–3} Neurodegeneration and loss of dopamine-producing neurons in the substantia nigra pars compacta is one of the hallmarks of PD pathology and leads to dopamine (DA) depletion in the striatum.^{4,5} On the basis of the classical model of basal ganglia function, dopamine release into the striatum fine-tunes basal ganglia output by modulating two opposing motor control circuits in the brain—the direct (striatonigral) and the indirect (striatopallidal) pathways.⁶ In the striatum, direct pathway medium spiny neurons expressing dopamine D1 receptors (D1-type MSN) are intermingled with indirect pathway MSN expressing dopamine D2 receptors (D2-type MSN). Loss of DA in PD is believed to cause hypoactivity in the direct and hyperactivity in the indirect pathways, which produces a net increase of inhibitory GABAergic output from the basal ganglia and suppresses movement in PD patients.⁶

Replacing DA with levodopa (L-DOPA), a prodrug of DA, is still the gold standard treatment to manage motor symptoms of PD.^{7,8} However, long-term use can result in significant dyskinesia and thus substantially decreases the quality of life of patients.^{9,10} Other dopaminergic therapies with clinical effectiveness have been developed: catechol-O-methyltransferase (COMT) inhibitors,¹¹ monoamine oxidase-B (MAO) inhibitors,¹² and dopamine receptor agonists,¹³ they but are associated with various side effects.¹⁴ Multiple non-dopaminergic therapies for PD have been developed,¹⁵ including the adenosine A2A antagonist istradefylline (KW6002), which achieved approval in the United States and Japan as an

Received: December 1, 2020

Table 1. Major SAR on the Right-Hand Side (RHS) Bicyclic Ring System



Analog	R ¹	R ²	X	EC ₅₀ ^a (μM)	Y _{max} % ^c
1				43	73
2a		H		14	110
2b		H		2.1	89
2c ^b		7-Me		16	90
2d		7-OMe		4.1	90
2e		7-F		1.2	90
2f		7-CN		0.174	107
2g		6-CONMe ₂		0.090	105
3a			7-aza	0.055	102
3b			6-aza	0.053	110

^aTR-FRET cAMP inverse agonist assay using a human GPR6 CHO-K1 cell line (Materials and Methods); EC₅₀ values are the means of at least two individual experiments with each concentration tested in triplicate. ^bMixture of two regioisomers (2:1). ^cEfficacy (Y_{max}) is normalized to the efficacy of a reference compound, which was validated to inhibit the apparent constitutive activity of GPR6 receptors expressed in cAMP TR-FRET assays (Supporting Information).

adjunctive therapy to L-DOPA.¹⁶ Deep brain stimulation (DBS) in the globus pallidus or subthalamic nucleus of the indirect pathway is FDA approved and significantly improves the motor symptoms of PD.^{1,17} Importantly, because of the localized placement of the DBS probes, it avoids modulating the direct pathway known to be a major driver of L-DOPA-induced dyskinesia (LID). Therefore, development of a drug that selectively targets the indirect pathway in PD could avoid invasive DBS procedures and provide therapeutic benefit without increased risk of drug-induced dyskinesia.

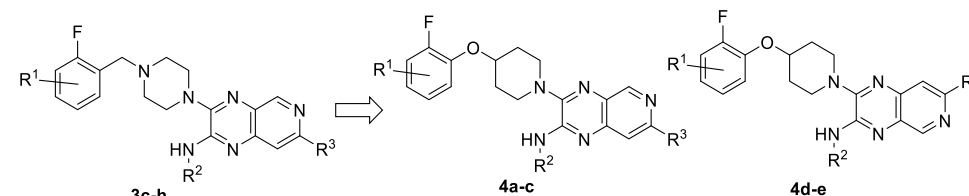
GPR6 is a highly constitutively active orphan G-protein coupled receptor,^{18–20} with highly restricted expression in the indirect pathway D2-type MSNs in the striatum²¹ and minimal expression in the direct pathway D1-type MSNs, other brain regions, and peripheral tissues. GPR6 receptors efficiently couple to Gs proteins in heterologous expression systems and constitutively stimulate adenylate cyclase activity and cyclic adenosine monophosphate (cAMP) accumulation in cells *in vitro*.^{18–20} cAMP levels are reduced in striatal tissue derived from GPR6 knock out mice, which is consistent with GPR6 Gs protein coupling and cAMP signaling *in vivo*.^{22,23} In contrast to GPR6, dopamine D2 receptors expressed in the indirect pathway D2-type MSN are Gi protein coupled and inhibit cAMP signaling.²⁴ We hypothesize that inhibition of GPR6 and D2 receptors coexpressed in the indirect pathway D2-type MSN antagonize each other with respect to cAMP modulation. Consequently, targeting GPR6 with antagonists or inverse agonists could be a novel non-dopaminergic treatment to improve motor symptoms in PD through selective modulation of the indirect pathway by compensating for the lack of DA acting on D2 receptors. In addition, pharmacological inhibition of GPR6 is expected to have only a low risk for drug-induced dyskinesia because of the restricted expression in striatal D2-

type MSN.^{25,26} The phenotype of GPR6 receptor knock out mice support a role of GPR6 receptors in basal ganglia function and its potential use as a PD drug target. They display a two-fold increased phosphorylation of Thr43 of the DARPP32 protein in the striatum, which is a key regulator of DA signaling. They also display increased locomotor activity and a reduced abnormal induced movement (AIM) in a dyskinesia PD rodent model.²³

Herein we report the discovery of the first potent and selective GPR6 inverse agonists and their pharmacological validation in preclinical PD behavioral animal models.

RESULTS AND DISCUSSION

A GPR6-selective high throughput screen (HTS) campaign was run to identify novel GPR6 inverse agonists as starting points for medicinal chemistry efforts. In total, 360 000 compounds were screened for inverse agonist activity in a GPR6-selective, cell-based time-resolved fluorescence resonance energy transfer (TR-FRET) cAMP assay using a stable and inducible CHO-K1-based cell line expressing human GPR6 receptor (see Materials and Methods). Only one very low-potency hit, compound 1 (Table 1), was identified in the screen and validated in a secondary full concentration–response repeat assay (EC₅₀ = 43 μM). Compound 1 did not modulate the baseline cAMP level or forskolin-stimulated cAMP levels in the uninduced CHO-K1-GPR6 cell line, which did not express GPR6 (data not shown). Furthermore, compound 1 did not modulate cAMP signaling in a cannabinoid receptor CB1-specific counterscreening assay (data not shown). Structure–activity relationship (SAR) optimization was initiated with the aim to improve the potency and druglike properties of compound 1 despite the fact that it contains a [1,2,5]-oxadiazole-containing bicyclic

Table 2. Optimization on the Pyrido[3,4-*b*]pyrazine Scaffold to Balance Selectivity and ADMET Properties


analogue	R ¹	R ²	R ³	EC ₅₀ ^a (nM)	selectivity over GPR3 (fold)	selectivity over GPR12 (fold)	P450 (2D6) pIC ₅₀	hERG binding % @10 uM	cLogP ^b
3c	5-Cl	c-Pr	H	29	638×	15×			3.8
3d	5-F	c-Pr	H	151			6.9	40	3.2
3e	4-F	c-Pr	H	39	21×	80×	7.3	40	3.2
3f	4-F	c-Pr	Me	29	14×	78×	5.4	23	3.3
3g	4-F	i-Pr	H	21	9×	14×			3.4
3h	4-F	i-Pr	Me	51	5×	19×	5.4	13	3.6
4a	4-F	c-Pr	Me	29	19×	105×	5.2	75	3.4
4b	4-F	i-Pr	Me	16	13×	27×	5.2	75	3.7
4c	4-F	i-Pr	CN	55	6×	13×			3.8
4d	4-F	c-Pr	Me	95	19×	105×	5.2		3.4
4e	4-F	i-Pr	Me	61	19×	47×	5.4	71	3.7

^aTR-FRET cAMP inverse agonist assay using a CHO-K1-based cell line; EC₅₀ values are the means of two or more individual experiments with each done in triplicate. ^bcLogP values are calculated with ChemAxon.

aromatic ring, which is a structural feature frequently found in pan-assay interference compounds (PAINS) that often show up as false positives in HTS.²⁷

Accordingly, our initial focus was to explore less problematic bicyclic ring systems with more vectors to explore for SAR and to remove the structural alert at the onset of the program. Fortunately, our first attempt to replace the five-membered oxadiazole ring with an unsubstituted phenyl ring was tolerated and even provided a modest improvement in potency (3-fold; EC₅₀ = 14 μM; **2a** in Table 1). This new quinoxaline scaffold served as the basis for further systematic SAR exploration. While it was found that other small alkyl amines were also accommodated as cyclopropyl replacements, the cyclopropylamine was superior in terms of both potency and physicochemical properties (data not shown) in this early SAR. Next, introduction of small alkyl or phenyl groups on any carbon of the piperazine ring was not tolerated (data not shown). Modification of the benzyl group with one or two substituents showed a more significant impact on the potency as demonstrated by the initial compound **2b** bearing a 2,5-dichlorophenyl ring (EC₅₀ = 2.1 μM) and providing a seven-fold improvement in potency compared to **2a**, likely as a result of increased lipophilic interactions of the protein–ligand complex.

However, the most significant functional potency improvement during the early phase of the project resulted from the modification of the quinoxaline phenyl ring. Introduction of a hydrophobic methyl group (**2c**) reduced the potency by eight-fold. Although the introduction of an electron-withdrawing F atom (**2e**) or the electron-donating OMe group (**2d**) was better tolerated, no sub-micromolar potency breakthrough was realized. In contrast, a strong electron-withdrawing group like CN (**2f**) or dimethyl amide (**2g**) was found to significantly enhance the potency to the 100 nM range. Incorporation of a nitrogen atom into the phenyl ring at either the 6 or 7 position (**3a** and **3b**) also boosted potency (50 nM), with no regiochemical preference observed between these two positions. In addition, this introduction of a ring nitrogen

provided the benefit of improved physicochemical properties, such as lower lipophilicity (cLogP), and higher lipophilic ligand efficiency (LLE), which are known to correlate with improved metabolic stability and solubility.

In order to further lower lipophilicity of **3a** and **3b** (cLogP > 4.5), we conducted an extensive SAR investigation on the more potent pyrido[3,4-*b*]pyrazine scaffold, focused on the western side of the molecule with the goal to replace the two very hydrophobic chlorine atoms. Gratifyingly, we found that replacement of the 2-chloro group on that phenyl ring with a fluorine atom was tolerated (**3c** in Table 2). In contrast, replacing both Cl atoms with F atoms at the 2 and 5 position decreased the potency by five-fold (**3d** in Table 2). Upon further investigation into the optimal substitution pattern on the benzyl moiety, we found that moving the 5-F atom to the 4 position (compound **3e**) was much preferred and provided potency below 50 nM. In addition, the lipophilicity of **3e** (cLogP = 3.2) was now within our acceptable range.

Additional pharmacological and physicochemical properties of compound **3e** are depicted in Table 3. In addition to the

Table 3. Pharmacological and Physicochemical Properties of Tool Compound **3e**

property	value
binding affinity K _i (nM)	7
functional EC ₅₀ (nM)	39
LLC-PK1-MDR1 A to B (nm/s)	160
P-gp efflux ratio	0.5
cLogP	3.2
CNS MPO	4.8

cAMP functional potency on GPR6 receptor, **3e** possesses strong binding affinity: K_i = 7.0 nM (*in vitro* competition binding assay using a tritium-labeled tracer compound; see Materials and Methods, and Table 3). Compound **3e** also exhibited high passive permeability and did not behave as a P-gp substrate as indicated by the low efflux ratio (ER) in the

LLC-PK1-MDR1 cell monolayer assay. On the basis of these *in vitro* pharmacology properties in combination with acceptable subcutaneous rodent PK (absorption and central uptake—data not shown), we were enabled to explore for the first time the effect of GPR6 inhibition on rodent behavior in pharmacodynamic PD models.

Haloperidol, a potent dopamine receptor D2 antagonist, activates striatal D2-type MSN of the indirect pathway, causing catalepsy in rats. GPR6 IAG 3e dose-dependently (0.1–30 mg/kg sc) reversed haloperidol-induced catalepsy (Figure 1a). This result suggests that inhibition of GPR6 reduces activity of the indirect pathway, which is expected to reduce inhibition of movement.

GPR6 knock out mice show similar sensitivity for haloperidol to induce catalepsy than wild-type mice (Figure 1b). However, compound 3e (30 mg/kg sc) was unable to

reverse haloperidol-induced catalepsy in GPR6 knock out mice, confirming that GPR6 receptor inhibition is mediating the efficacy of GPR6 IAG 3e to reverse catalepsy in this PD model. As expected, the adenosine receptor A2A antagonist KW6002 was able to reverse haloperidol-induced catalepsy in both wild-type and GPR6 knock out mice (Figure 1b). Together, these results support the concept that GPR6 IAG reduce activity of the indirect pathway and might have potential as a therapeutic to treat motor symptoms of Parkinson's disease.

With the results from the catalepsy experiment, our confidence in the mechanism of action as described earlier had increased significantly. Therefore, we initiated lead optimization of compound 3e by posing the question: What properties of the tool compound need to be improved in order to develop the candidate suitable for clinical development? This analysis revealed numerous areas to focus the lead optimization efforts on, and most of them could be addressed by applying established medicinal chemistry strategies:

- strong cytochrome P450 inhibition (mostly isoform 2D6): likely a result of the exposed eastern N atom
- poor metabolic stability in human microsomes and hepatocytes leading to unacceptable human PK predictions
- putative risk for time-dependent clearance inhibition resulting from the cyclopropyl amine^{28,29}
- insufficient selectivity over the closest neighbors GPR3 and GPR12, two G-protein coupled receptors in the same GPCR subfamily as GPR6^{30–32}

With the above mitigation strategies, we embarked on a few “quick wins”. Strong inhibition of one cytochrome P450 isoform (2D6) from 3e (pIC₅₀ = 7.3) was diminished through the strategic introduction of a methyl group on the carbon adjacent to the pyridyl nitrogen (3f), minimally impacting cLogP. Unfortunately, this modification also led to the further erosion of the already poor selectivity ratios over GPR3 and GPR12. Our initial goal was to keep a minimal 30-fold selectivity, ideally higher, but with the very poor selectivity observed from many of our pyridopyrazine analogues especially against GPR3, this fused bicyclic scaffold was deprioritized. Moreover, “quick win” attempt number two failed for the same reason—the introduction of an isopropylamine group (compound 3g and 3h, Table 2) to replace the cyclopropyl amine (a potential structural alert) also afforded a loss of selectivity revealed by pairwise comparison with the corresponding cyclopropylamine (compound 3e).

As these initial tactics had not proven successful, we switched our focus toward improving metabolic stability. A metabolite identification (Met ID) study revealed the major route of oxidative metabolism takes place at the benzyl-piperazine subunit via benzylic oxidation and subsequent N-debenzylation (data not shown). Among many structural iterations, it was found that a phenolic-piperidine replacement was tolerated and maintained potency, and importantly, this structural change appeared to be feasible to reduce oxidative metabolism as demonstrated by comparing human microsomal turnover rates of selected pairs such as 3f and 4a (74 mL/min/kg over 45 mL/min/kg, respectively). The improved metabolic stability of compounds containing the phenolic-piperidine vs the benzyl-piperazine was consistent throughout the program.

Interestingly, a slight improvement in the selectivity profiles versus GPR3 and GPR12 was also observed in pairwise

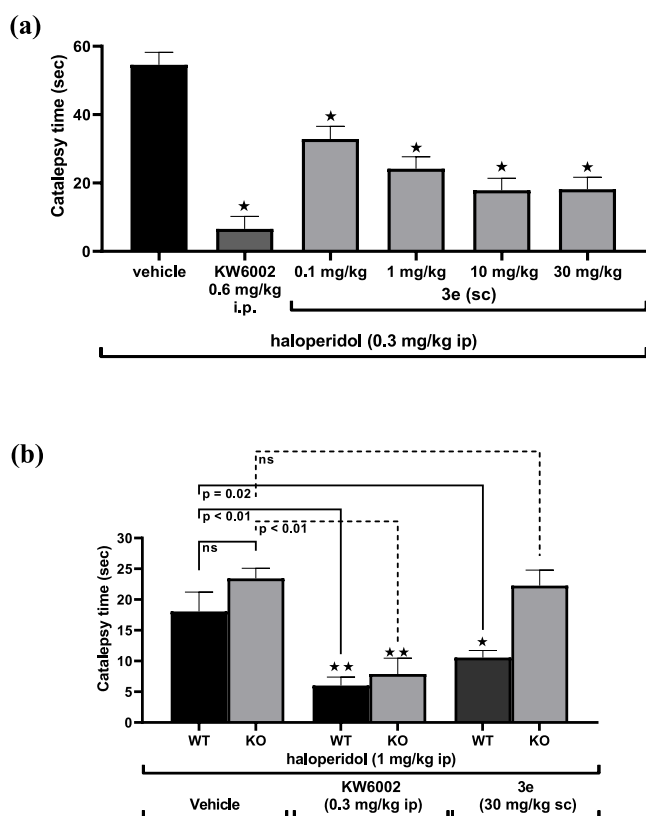
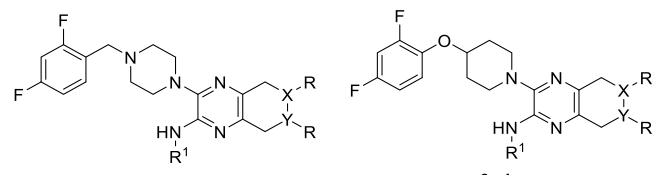


Figure 1. Studies on compound 3e in a haloperidol-induced catalepsy model. (a) Compound 3e reverses haloperidol-induced catalepsy in male rats. Haloperidol-induced catalepsy was measured 120 min after dosing Sprague-Dawley rats ($n = 9–10$ per group) at the same time with haloperidol (1 mg/kg, ip) and either vehicle (10% DMSO, 0.5% methylcellulose) or compound 3e (0.1, 1, 10, and 30 mg/kg sc) or positive control compound KW6002 (0.6 mg/kg ip; adenosine A2A antagonist) treatments. (b) Compound 3e reverses catalepsy in wild-type (WT) but not in male GPR6 knock out (KO) mice. Haloperidol-induced catalepsy was measured in wild-type (C57BL/6J) and GPR6 knock out mice 120 min after dosing animals at the same time ($n = 6$ per group) with haloperidol (1 mg/kg, ip) and vehicle (10% DMSO, 0.5% methylcellulose) or after dosing at the same time with haloperidol and either compound 3e (30 mg/kg sc) or positive control compound KW6002 (0.3 mg/kg ip; adenosine A2A antagonist). Applied statistics: one-way ANOVA using Dunnett's post hoc tests, significant effect of genotype difference or treatment as indicated: * $p < 0.05$ and ** $p < 0.01$.

Table 4. Saturation of the Right-Hand Side (RHS) Pyridine Ring Leading to the Lead Compound 6h



analogue	X-R	Y-R	R ¹	EC ₅₀ (nM) ^a	selectivity over GPR3 (fold)	selectivity over GPR12 (fold)	P450 (2D6) pIC ₅₀	hERG binding % @ 10 μM	cLogP ^c
5a	CH ₂	-NCOMe	i-Pr	27	25×	30×	5.4	11	2.3
5b	CH ₂	-NCOEt	i-Pr	30	20×	16×	<5.0		3.0
5c	CH ₂	-NSO ₂ Me	i-Pr	27	7×	8×	5.7 ^b		1.8
6a	-NCOMe	CH ₂	i-Pr	96	15×	15×	4.5	30	2.3
6b	-NCOMe	CH ₂	c-Pr	34	40×	120×	<5.2	58	2.0
6c	CH ₂	-NH	i-Pr	100	1.6×	16×	5.4	41	2.7
6d	CH ₂	-NMe	i-Pr	89	21×	69×	<5.0	36	3.1
6e	CH ₂	-NSO ₂ Me	i-Pr	65	15×	26×	<5.0		1.8
6f	CH ₂	NCOOMe	i-Pr	158	190×	34×	5.1	10	3.0
6g	CH ₂	-NCOMe	c-Pr	43	52×	272×	<5.0	81	2.0
6h	CH ₂	-NCOMe	i-Pr	34	110×	97×	5.4	69	2.3

^aTR-FRET cAMP inverse agonist assay using a human GPR6 CHO-K1 cell line (Materials and Methods); EC₅₀ values are the means of at least two individual experiments with each concentration tested in triplicate. ^bOver P450 isoform 1A2. ^ccLogP values are calculated with ChemAxon.

comparisons for the phenolic-piperidines (4a and 3f, and 4b and 3h; Table 2). Expanding this SAR briefly to explore additional potential selectivity gains, the pyridyl nitrogen was moved from position 6 to 7 (4d and 4a, and 4e and 4b), which did not afford a change in selectivity, unfortunately. The introduction of the electron-withdrawing group CN (4c) at the carbon adjacent to the pyridyl nitrogen decreased the selectivity versus both GPR3 and GPR12.

The SAR described in Table 2 seemed to be moderately promising; however, another concerning liability was introduced and had to be carefully monitored. As shown in Table 2, hERG binding affinity was significantly increased for compounds (4a,b and 4e).

After only limited success was achieved thus far, we explored more incisive modifications on the bicyclic aromatic ring system. We hypothesized that lowering lipophilicity and increasing fraction sp³ of the rather flat and highly aromatic system could be beneficial to addressing some key areas for optimization on a more overall compound quality and balanced property basis, decreasing promiscuity and increasing chances of clinical success.^{33,34} Accordingly, compounds 5a–c and 6a–i with saturation of the RHS pyridine ring were synthesized. We anticipated that removal of the exposed N atom and the increased three-dimensional character would lead to decreased CYP2D6 inhibition, decreased hERG activity, and improved selectivity over GPR3 and GPR12. The results are summarized in Table 4.

After saturation of the aromatic bicyclic ring system in combination with the LHS piperazine ring motif, the newly generated basic nitrogen was masked as either an amide or a sulfonamide (5a–5c, Table 4). Encouragingly, all compounds exhibited potency levels in the desired range and, indeed, demonstrated lower hERG binding in many compounds as hypothesized earlier (5a). Moreover, 5a showed a 2–3-fold improvement in selectivity over both GPR3 and GPR12. However, sterically more demanding N-masking groups were detrimental to the selectivity.

The next important breakthrough in the project was achieved when the newly developed western phenolic-

piperidine subunit was combined with the new partially saturated RHS core, leading to a number of notable improvements. To our surprise, 6b (R¹ = cyclopropyl) exhibited much improved selectivity, 40-fold over GPR3 and 120-fold over GPR12. Although the selectivity trend of the cyclopropylamine over isopropylamine was evidenced again by comparing 6b with 6a, it was difficult to manifest a clear selectivity strategy lacking a more reliable SAR trend. With this observation, we attempted a similar idea as described for the aromatic analogues from Table 3 and also synthesized 6g and 6h as the regioisomers of 6a and 6b, respectively. In contrast to the aromatic analogues, a significant selectivity improvement was achieved. Both 6g and 6h showed selectivity values for both GPR3 and GPR12 well above our criteria of 30 fold. Our investigation on the RHS saturated ring was expanded, but none of these attempts were successful. These efforts either led to the loss of potency, like 6c (unmasked nitrogen), 6d (methylated nitrogen), and 6f (N masked as a carbamate), or were not tolerable to the selectivity, like 6e (masked as sulfonamides). After a careful review of all relevant data, we realized that compound 6h was the most promising of all late-stage lead optimization contenders, eliminating all the concerns that were identified with compound 3e. Compound 6h was selected as the project's first advanced lead and *in vivo* tool compound. A snapshot of the relevant data contributing to the selection process of compound 6h is depicted in Tables 5 and 6. Summarizing a few key features, 6h exhibited 16 nM binding affinity in competitive radioligand binding assays, similar to its functional potency in cell-based cAMP TR-FRET assays (EC₅₀ = 34 nM). LLC-PK1-MDR1 efflux assays indicated a high brain permeability, and robust metabolic stability was observed in human hepatocyte (hHep) stability assays. A follow-up hERG functional assay gave IC₅₀ = 6.2 μM, consistent with its hERG binding affinity.

As a result of the identification of 6h, the project objectives were revised, leading to a parallel three-prong approach:

- Objective 1: initiate the development of a quantitative receptor occupancy (RO) assay, either *in vivo* or *ex vivo*

Table 5. Summary of Other Key Properties for Lead Compound 6h

property	6h
binding affinity K_i (nM)	16
functional EC_{50} (nM)	34
selectivity over GPR3 (fold)	110×
selectivity over GPR12 (fold)	97×
logD	4.5
LLE (logEC ₅₀ -clogP)	5.0
LLC-PK1-MDR1 A to B (nm/s)	160
P-gp efflux ratio	0.7
HLM, Cl_{int} (mL/min/kg)	45
HHep, Cl_{int} (mL/min/kg)/fu (%)	5.7/16%
hERG screen (Cerep) functional IC_{50}	6.2 μ M
dog CV (CorDynamics) no findings@	30 mg/kg p.o.
dog C_{max} (total/free) at 30 mpk	11.0 μ M/11 nM

- Objective 2: initiate all required *in vivo* tolerability, pharmacology, and pharmacokinetic studies with **6h** and explore the feasibility of generating a candidate selection package
- Objective 3: continue the lead optimization to mitigate for a potential failure of **6h**

Executing on the newly devised research plan, objective 1 started with the search for a suitable tool tracer compound to measure RO *in vivo*. First, we focused on developing an isotope (label)-free LC-MS/MS-based *in vivo* RO method for GPR6 receptors in rodents, based on previously reported successful strategies.³⁵ The use of LC-MS/MS techniques to quantify levels of unlabeled tracer compound in discrete brain regions expressing the target of interest offers an attractive alternative to assess real *in vivo* RO, circumventing the need to identify and generate radiolabeled tracer, reducing associated costs and increasing turnaround time. First, we applied compound selection criteria (e.g., high potency, high selectivity, rapid brain uptake, and rapid wash out),³⁶ dosed animals intravenously (i.v.), dissected brain regions, and screened for brain penetrant compounds that demonstrated strong enrichment in the striatum compared to the cerebellum, using LC-MS/MS-based quantification methods. A suitable GPR6 tracer compound is expected to show a several fold enrichment in the striatum due to the high expression of GPR6 in striatal D2-type MSN, compared to nonspecific binding in the cerebellum, a brain region that lacks significant expression of GPR6 receptors. The time course of tracer enrichment and knowledge of the lowest tracer dose that achieved largest fold enrichment are additional criteria to be considered for tracer selection and validation. Most importantly, after successful optimization and assay development, the enrichment of a suitable tracer can be blocked by predosing the test compound at therapeutically relevant doses, which allows quantification of receptor occupancy for the test compound.

As shown in Figure 2a, the selected cold tracer molecule RL-338 achieved baseline enrichment of roughly nine-fold in

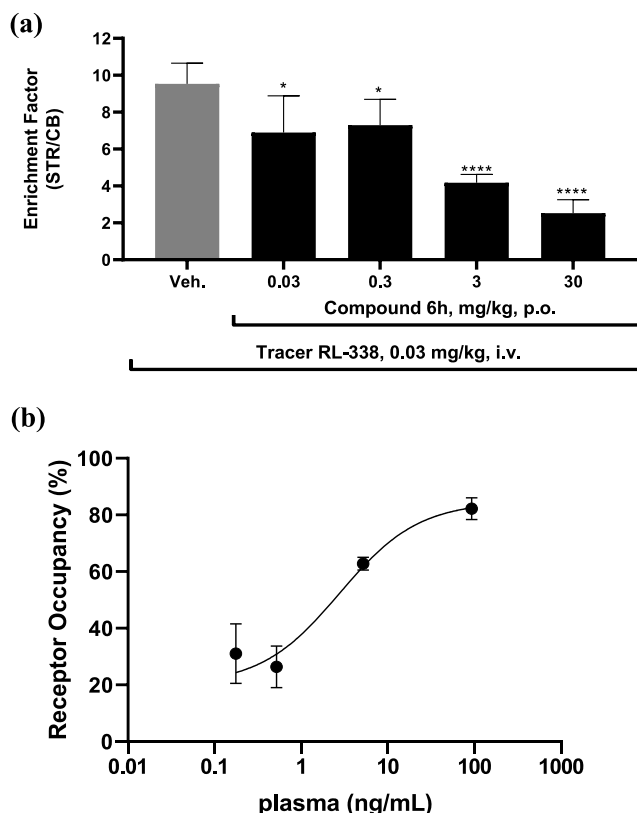


Figure 2. In vivo label-free LC-MS/MS-based GPR6 receptor occupancy (RO) of lead compound **6h** in male Sprague-Dawley rats. (a) GPR6 IAG tracer compound RL-338 (0.04 μ g/kg, i.v.) accumulates nine-fold in the rat striatum (STR), a brain region expressing a high level of GPR6, in comparison to the cerebellum (CB), a brain region without GPR6 expression (90 min post dosing). Compound **6h** (0.03, 0.3, 3 and 30 mg/kg, p.o.) dose-dependently reduced striatal enrichment of tracer RL-338 compared to vehicle (Tween-80, 0.5% methylcellulose) 90 min post dosing—an *in vivo* measure of isotope-free GPR6 receptor occupancy. (b) Correlation of compound **6h** plasma exposure and striatal receptor occupancy using *in vivo* label-free RO method (compound **6h** Occ_{50} (plasma) = 2.8 ng/mL). Data are mean \pm s.e.m. ($n = 5$ per group) after 90 min postinjection of **6h**; * $P < 0.05$, **** $P < 0.0001$ vs vehicle.

mouse striatum over background tissue (cerebellum) where GPR6 is not present. Striatal enrichment of compound RL-338 was absent in GPR6 knock out mice, confirming the high specificity of RL-338 for GPR6 receptor binding *in vivo* (data not shown). Rewardingly, predosing **6h** (0.03, 0.3, 3, 30 mg/kg; p.o.) achieved a clear and dose-dependent blockage of the striatal enrichment of tracer RL-338, confirming that **6h** efficiently occupies GPR6 receptors *in vivo* (Figure 2b). To

Table 6. Pharmacokinetic Properties of Lead Compound 6h in Male Sprague-Dawley Rats

route	dose (mg/kg)	subject ($n = 3$)	AUC (0 – τ) (h*ng/mL)	AUC (0 – ∞) (h*ng/mL)	CL (mL/min/kg)	V_{dss} (L/kg)	term $t_{1/2}$ (h)
i.v.	1	mean	339	341	49.7	3.68	1.12
		SD	53	53	7.9	0.37	0.12
route	dose (mg/kg)	subject ($n = 3$)	C_{max} (ng/mL)	T_{max} (h)	F		
p.o.	2	mean	62.5	1.00	0.50		
		SD	9.9	0.87	0.09		

the best of our knowledge, this is the first time that the successful application of the isotope-free LC-MS/MS RO method is reported for an orphan GPCR. A plasma exposure of **6h** (2.8 ng/mL; 6.1 nM) was required to achieve 50% maximal GPR6 receptor occupancy (Occ50). To further study compound **6h** receptor occupancy, we additionally developed an ex vivo GPR6 receptor occupancy assay, using a tritium-labeled form of our tracer compound RL-338 (Supporting Information). After oral dosing, compound **6h** dose-dependently achieved ex vivo-based RO in rats with a plasma Occ50 of 3.4 ng/mL (7.5 nM), which is similar to the Occ50 determined using the LC-MS/MS-based RO method (data not shown). Both methods together confirmed that compound **6h** efficiently achieved RO in vivo.

Executing on objective 2, compound **6h** did not show any signals in our internal collection of *in vitro* safety assessments including mutagenicity. To derisk the moderate hERG signal, a cardiovascular study in dogs was conducted, and no adverse effects (AEs) were detected at a dose of 30 mpk. Likewise, 14-day toxicological studies in rat and dog did not unveil any findings at the highest doses of 300 mpk and 30 mpk in rats and dogs, respectively, despite achieving very high total plasma.

To further understand the efficacy of GPR6 inhibition to treat the motor symptoms of PD, we focused on testing our lead compound **6h** in the bilateral 6-OHDA-lesion PD model that exhibits the loss of dopaminergic neurons in the substantia nigra and dopamine depletion in the striatum, reflecting one of the pathological hallmarks of Parkinson's disease. Rats with bilateral 6-OHDA lesions develop loss of mobility (Figure 3) and are used as preclinical behavioral *in vivo* models to study compounds for efficacy to treat the motor symptoms in PD.³⁷

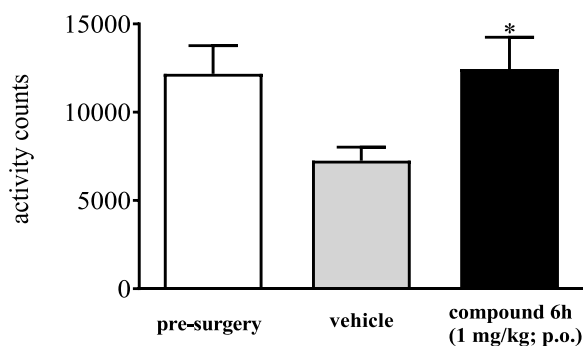


Figure 3. Compound **6h** shows anti-Parkinsonian efficacy in the bilateral 6-OHDA-lesioned rat model of Parkinson's disease. 6-OHDA-lesioned female animals are dosed with vehicle (0.5% methylcellulose) or compound **6h** (1 mg/kg, p.o.). Animals are placed in automated activity monitors for 3 h post dosing to assess mobility. The pen field activity of unperturbed study animals before the introduction of a bilateral 6-OHDA lesion is shown as control. Collected data are mean ± s.e.m. ($n = 10$ per group) of total counts over 3 h. * $P < 0.05$ vs vehicle; repeated measures one-way ANOVA followed by Newman-Keuls test.

Oral dosage (1 mg/kg) of compound **6h** restored mobility of 6-OHDA-lesioned animals to presurgery level (Figure 3). This result is consistent with the proposed mechanism of action: inhibition of GPR6 receptors normalizes dopamine-like cAMP signaling in dopamine D2 type MSNs and reduces hyperactivity in the indirect pathway in the striatum. The results of our initial *in vivo* pharmacology studies characterizing selective GPR6 IAG **3e** and **6h** in the catalepsy model

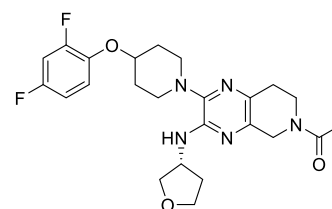
and the 6-OHDA-lesion PD model, respectively, provide first preclinical evidence that efficient GPR6 inhibition *in vivo* could represent a novel mechanism to treat motor symptoms in Parkinson's disease. A manuscript expanding the study of GPR6 biology and the pharmacological characterization of compound **6h** is in preparation (unpublished).

The commitment to objective 3 led to the discovery of compound **6i**, which has many of the favorable druglike properties of **6h** but with some advantages such as lower lipophilicity and higher *in vivo* toxicity margins. Therefore, **6i** was selected for candidate development over **6h**. Compound **6i**, now named CVN424, is currently in phase 2 clinical development to treat motor symptoms in PD by Cerevance, Inc. A manuscript describing the preclinical *in vitro* and *in vivo* pharmacological characterization of CVN424 (**6i**) is in press.³⁸

A selection of key data is summarized in Table 7 for compound **6i**.

Table 7. Summary of Key *In Vitro* ADMET and Pharmacological Properties of Lead Compound **6i (CVN424)**

property	6i
binding affinity K_i (nM)	9.4
functional EC_{50} (nM)	38
selectivity over GPR3 (fold)	265×
selectivity over GPR12 (fold)	68×
logD	3.6
LLE (log EC_{50} -cLogP)	5.8
LLC-PK1-MDR1 A to B (nm/s)	170
P-gp efflux ratio	0.7
HLM, Cl_{int} (mL/min/kg)	62
HHep, Cl_{int} (mL/min/kg)/fu (%)	48/51%
hERG Screen (Cerep) functional IC_{50}	3.5 μ M

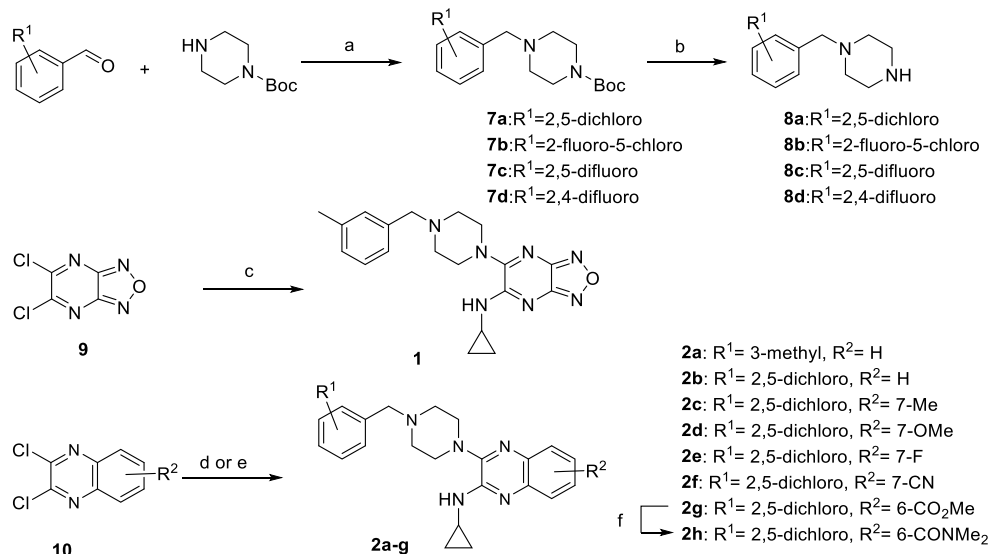


6i (CVN424)

CONCLUSION

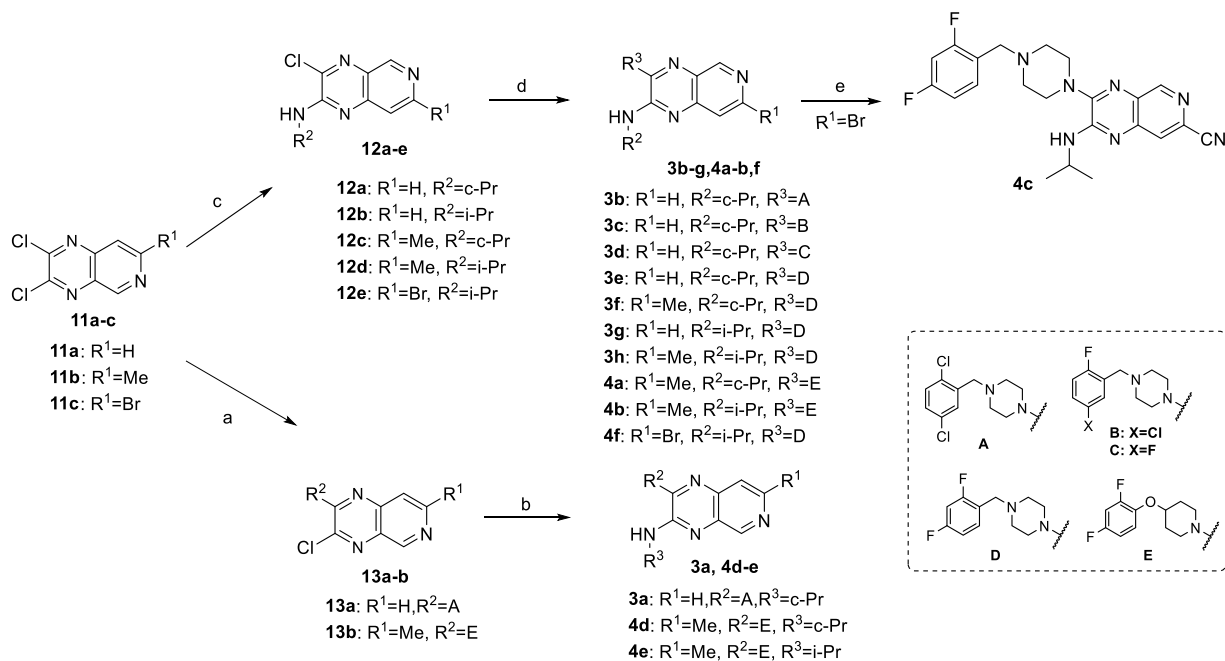
Pharmacological modulation of the indirect pathway in Parkinson's disease is a novel therapeutic strategy to reduce motor deficits in PD, without the risk of developing drug-induced dyskinesia. GPR6 is an orphan G-protein coupled receptor, with highly restricted expression in dopamine receptor D2-type medium spiny neurons (MSNs) of the indirect pathway, which triggered our interest to explore GPR6 as a novel non-dopaminergic drug target for PD. We started our SAR optimization campaign with a weak HTS hit **1** ($EC_{50} = 43 \mu$ M) and were able to achieve a 1000-fold boost in functional potency by introduction of electron density reducing heteroatom features on the bicyclic aromatic ring system. Other major issues, including P450 enzyme inhibition, poor selectivity over GPR3 and GPR12, and high lipophilicity were simultaneously overcome by the partial saturation of the RHS bicyclic aromatic ring system. We identified multiple GPR6 IAG compounds suitable for pharmacological validation

Scheme 1. Synthesis of Compounds 2a–g^a



^a Reagents and conditions: (a) NaBH(OAc)₃, DCE, rt; (b) HCl, dioxane, rt; (c) (i) cyclopropylamine, DIPEA, DCM, 0 °C; (ii) 1-(3-methylbenzyl)piperazine, DIPEA, rt. (d) (i) cyclopropylamine, dioxane, 80 °C; (ii) 1-(3-methylbenzyl)piperazine or **8a**, dioxane, 150 °C; for **2a–e** and **2g**; (e) (i) **8a**, DIPEA DCM, rt; (ii) cyclopropylamine, DIPEA, dioxane, 100 °C, for **2f**; (f) (i) **2g**, KOH, MeOH, rt; (ii) Me₂NH, HATU, DIPEA, DMF.

Scheme 2. Synthesis of Compounds 3a–h and 4a–f^a



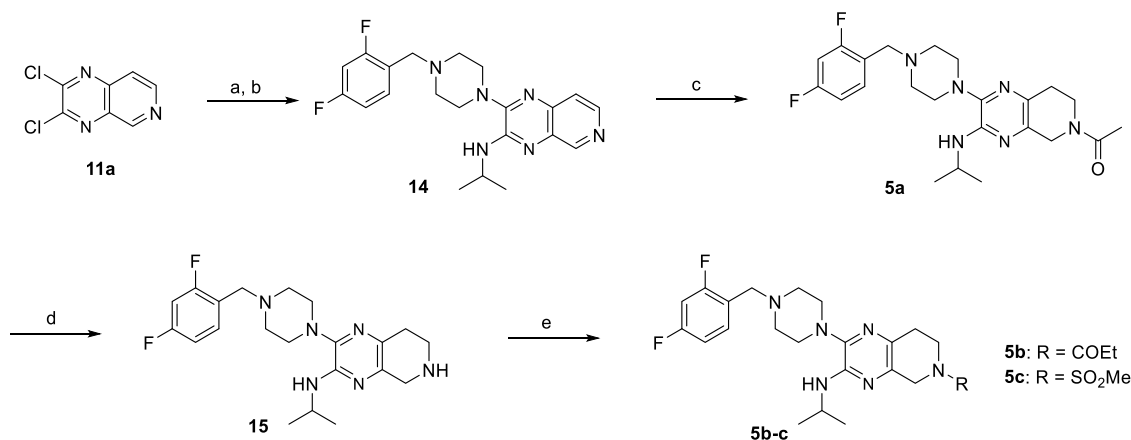
Reagents and conditions: (a) **8a** or 4-(2,4-difluorophenoxy)piperidine, DIPEA, DCM, 0 °C; (b) cyclopropylamine or isopropylamine, DIPEA, dioxane, 110 °C in a sealed tube; (c) cyclopropylamine or isopropylamine, DIPEA dioxane or DCM, 0 °C; (d) **8a**, **8b**, **8c**, **8d**, or 4-(2,4-difluorophenoxy)piperidine, DIPEA, dioxane, 80 °C; (e) **4f**, 1,1'-bis(diphenylphosphino) ferrocene, Pd₂(dba)₃, Zn(CN)₂, NMP, 120 °C.

of our therapeutic hypothesis in behavioral PD models. Tool compound **3e** reversed haloperidol-induced catalepsy, and early lead compound **6h** demonstrated anti-parkinsonian efficacy in the bilateral 6-OHDA-lesioned PD model, providing for the first-time experimental evidence that pharmacological inhibition of GPR6 *in vivo* could be a feasible non-dopaminergic therapeutic strategy to reduce motor deficits in human PD patient. Compound **6i**(CVN424) has successfully progressed through clinical phase I safety testing and is

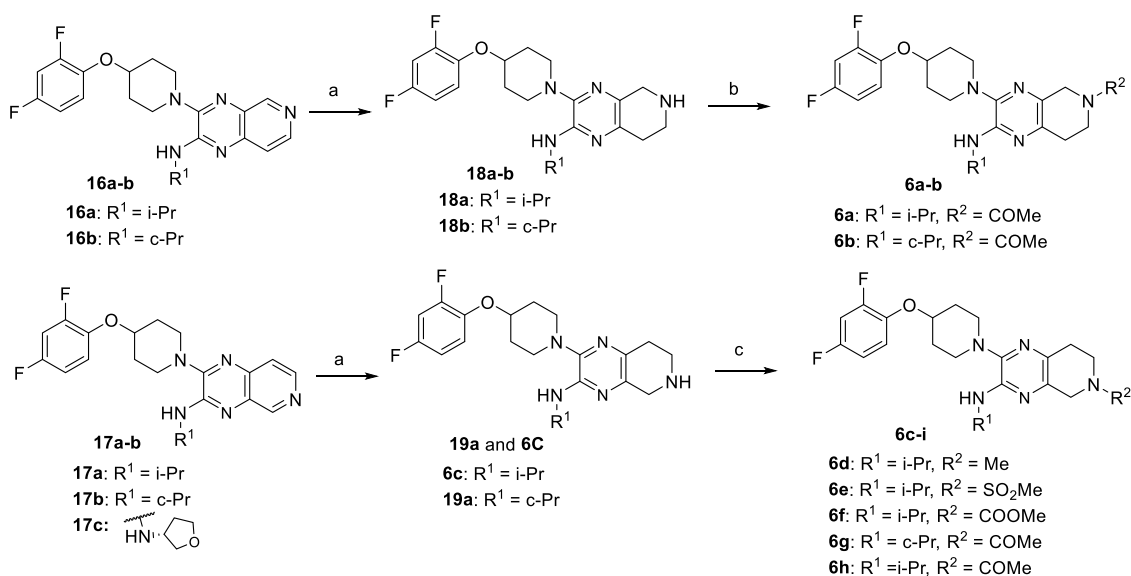
currently in clinical phase II trials to validate the therapeutic efficacy to treat motor symptoms in PD.

■ SYNTHESIS

Some common amine intermediates were prepared via a reaction sequence of reductive amination and subsequent Boc deprotection with HCl as shown in [Scheme 1](#). The initial hit **1** was resynthesized by sequentially reacting **9** with cyclopropyl-

Scheme 3. Synthesis of Compounds 5a–c^a

^aReagents and conditions: (a) (a) **8d**, DIPEA, DCM, 0 °C; (b) isopropylamine, DIPEA, dioxane, 100 °C in a sealed tube; (c) Ac₂O, H₂, 10% Pd/C, acetone/dioxane, 45 °C; (d) NaOH, MeOH, 65 °C; (e) propionic anhydride or MeSO₂Cl, DIPEA, DCM, 0 °C.

Scheme 4. Synthesis of Compounds 6a–i^a

^aReagents and conditions: (a) (i). BnBr, MeCN, 80 °C; (ii). NaBH(OAc)₃, DCM, rt; (iii). H₂, Pd/C, MeOH, rt; (b) **18a** or **18b**, Ac₂O, DIPEA, DCM, 0 °C to rt; (c) **19a** or **6c**, MeSO₂Cl or Ac₂O or MeO₂CCl, DIPEA, DCM, 0 °C to rt.

amine and then 1-(3-methylbenzyl)piperazine (commercially available) at 0 °C in a one-pot reaction.

Intermediates **10** with different substituents (R² = H, 7-Me, 7-OMe, 7-F and 6-CO₂Me) underwent one S_NAr reaction with cyclopropylamine, followed by a second S_NAr reaction with 1-(3-methylbenzyl)piperazine or **8a** to afford compounds **2a–e** and **2g**. The different electron-withdrawing or -donating effect of the substituents on the phenyl ring resulted in different regioselectivities during the first S_NAr reaction. **2C** (7-Me) was obtained as a mixture of two regioisomers (2:1 ratio). In contrast, **2e** (7-F) was separated as one single isomer, but it is likely that the other regioisomer was lost during the purification process. **2d** with a strong electron-donating methoxy group and **2g** with a strong electron-withdrawing ester group were afforded as one single observed isomer; however, the directing effect of these two substituents for the regioselectivity is opposite during the first S_NAr reaction. Ester **2g** was hydrolyzed to the corresponding acid, which then reacted with dimethylamine to provide amide compound **2h**.

By following the same directing effect as the ester group, **2f** (7-CN) was prepared as the only isomer by reversing the reaction order of the two S_NAr reactions, starting with **8a** first.

Compounds **3a–h** and **4a–f** were prepared as shown in Scheme 2, in which the presence of the pyridine nitrogen (**11a–c**) also played a critical directing effect during the first S_NAr reaction for the synthesis of **12a–e** and **13a–b** when the reaction temperature and addition rate of the corresponding amine were carefully controlled. The second S_NAr reaction with corresponding amines gave rise to **3a–h**, **4a–b**, and **4d–f**, respectively. Palladium-catalyzed cyanation with Zn(CN)₂ based on substrate **4f** afforded final compound **4c** (**10**).

Intermediate **14** was constructed with both LHS amines via the same reaction sequence as **3a**, but the second S_NAr reaction with isopropylamine was significantly facilitated by adding KF as a promoter. The pyridine ring in the bicyclic ring system was then saturated after activation with acetic anhydride and *in situ* hydrogenation catalyzed by palladium to afford intermediate **5a** (**11**), which was readily hydrolyzed to the corresponding

secondary amine **15** by treating it with sodium hydroxide in MeOH at 65 °C. The resulting amine was reacted with either propionic anhydride or methanesulfonyl chloride to provide **5b** and **5c**, respectively.

As for the preparation of **6a–i** (Scheme 4), it also requires a saturation process on the pyridine ring. A two-step reaction sequence (benzylation followed by reduction with sodium triacetoxyborohydride) was developed to saturate the pyridine ring in this case (12–13). This optimized two-step procedure proved to be a more practical and scalable process in comparison to the one-pot reaction as described in Scheme 3. The subsequent debenylation under hydrogenation conditions afforded common secondary amine intermediates **6c**, **19a**, **18a–b**, with no purification needed over three steps. Final compounds **6a–i** were generated from the respective secondary amines using methylation, acylation, or sulfonation reaction conditions.

MATERIALS AND METHODS

General Methods. All reagents and solvents were purchased from commercial suppliers and used without purification unless otherwise noted. All reactions were performed at ambient temperature and in anhydrous solvents unless otherwise noted. Flash chromatography was performed on ISCO CombiFlash with prepacked silica gel columns and eluted with ethyl acetate in heptane. Preparative HPLC was performed on a Shimadzu LC-8A (UV/vis: SPD-20A; Software: LCSolution) with a Phenomenex Gemini C18, 5 μ m, ID 30 \times 100 mm column using either acid (0.1% TFA) or base (0.1% NH_4OH) modified MeCN/ H_2O gradients. ^1H NMR spectra were recorded on a 500 or 400 MHz Bruker instrument. Chemical shifts are expressed in parts per million (ppm) δ relative to residual solvent as an internal reference. The mass spectra were obtained using liquid chromatography mass spectrometry (LC-MS) on an Agilent 1260 Infinity instrument using electrospray ionization (ESI). All test compounds showed >95% purity as determined by LC-MS. All animal experiments performed in the manuscript were conducted in compliance with institutional guidelines.

Synthesis of N-Cyclopropyl-6-(4-(3-methylbenzyl)piperazin-1-yl)-[1,2,5]oxadiazolo[3,4-b]pyrazin-5-amine (1). To a solution of 5,6-dichloro-[1,2,5]oxadiazolo[3,4-b]pyrazine (200 mg, 1.05 mmol, 1.0 equiv) in DCM (5.0 mL) were added DIPEA (547.2 μ L, 3.14 mmol, 3.0 equiv) and cyclopropanamine (59.79 mg, 1.05 mmol, 72.56 μ L, 1 equiv). The mixture was stirred at 0 °C for 2 h. 1-(*m*-Tolylmethyl)piperazine (241.6 mg, 1.26 mmol, 1.2 equiv) was then added, and stirring was continued for 3 h at 20 °C. The mixture was concentrated under reduced pressure, and the resulting residue was purified by prep-HPLC (column: Boston Prime C18 150 \times 30 mm \times 5 μ m; mobile phase: [water (0.05% $\text{NH}_3\text{H}_2\text{O}$ + 10 mM NH_4HCO_3)-ACN]; B%: 55–85%, 7 min) to give N-cyclopropyl-5-[4-(*m*-tolylmethyl)piperazin-1-yl]-[1,2,5] oxadiazolo[3,4-b]pyrazin-6-amine (100.7 mg, 25.8% yield) as a white solid. ^1H NMR (400 MHz, CDCl_3) δ ppm 7.21 (t, J = 7.5 Hz, 1H), 7.14–7.06 (m, 3H), 5.88 (br s, 1H), 3.53 (s, 2H), 3.47–3.36 (m, 4H), 2.98 (dt, J = 3.4, 7.1 Hz, 1H), 2.61 (br d, J = 4.4 Hz, 4H), 2.34 (s, 3H), 1.04–0.95 (m, 2H), 0.69–0.57 (m, 2H); ESI-MS calcd for $\text{C}_{19}\text{H}_{23}\text{N}_7\text{O}$ [$\text{M} + \text{H}$] $^+$ = 365.20; found 366.1.

Synthesis of N-Cyclopropyl-3-(4-(3-methylbenzyl)piperazin-1-yl)quinoxalin-2-amine (2a). Step 1: A solution of 2,3-dichloroquinoxaline (400 mg, 2.010 mmol), cyclopropanamine (149 mg, 2.61 mmol), and DIPEA (526 μ L, 3.01 mmol) in dioxane (2871 μ L) was heated at 80 °C for 2 days. The solvent was removed under reduced pressure, and the residue obtained was purified by silica gel column chromatography (10–40% EtOAc/hexanes) that afforded 3-chloro-N-cyclopropylquinoxalin-2-amine as a light yellow solid. ^1H NMR (400 MHz, CDCl_3) δ ppm 7.79 (br d, J = 7.9 Hz, 2H), 7.58 (br t, J = 7.6 Hz, 1H), 7.39 (br t, J = 7.7 Hz, 1H), 5.72 (br s, 1H), 3.01–2.91 (m, 1H), 0.93 (br d, J = 6.8 Hz, 2H); ESI-MS calcd for $\text{C}_{11}\text{H}_{10}\text{ClN}_3$ [$\text{M} + \text{H}$] $^+$ = 219.06; found: 219.9.

Step 2: A solution of 3-chloro-N-cyclopropylquinoxalin-2-amine (30 mg, 0.137 mmol), 1-(3-methylbenzyl)piperazine (39.0 mg, 0.205 mmol), and N-ethyl-N-isopropylpropan-2-amine (0.072 mL, 0.410 mmol) in dioxane (0.25 mL) was heated at 150 °C overnight. HPLC purification afforded the title compound **2a** (30% yield) as a white solid. ^1H NMR (400 MHz, CDCl_3) δ 7.71 (br t, J = 8.7 Hz, 2H), 7.42 (br t, J = 7.5 Hz, 1H), 7.35–7.28 (m, 1H), 7.24–7.18 (m, 1H), 7.18–7.11 (m, 2H), 7.07 (br d, J = 7.1 Hz, 1H), 5.51 (br s, 1H), 3.55 (s, 2H), 3.22 (br s, 4H), 2.91 (dt, J = 3.0, 6.6 Hz, 1H), 2.61 (br s, 4H), 2.35 (s, 3H), 0.95–0.84 (m, 2H), 0.61–0.52 (m, 2H); ESI-MS calcd for $\text{C}_{23}\text{H}_{27}\text{N}_5$ [$\text{M} + \text{H}$] $^+$ = 373.23, found: 374.1.

Using similar reaction conditions as described above, and utilizing intermediates prepared as described above or commercially available piperazines, the following compounds were synthesized, and purified by either HPLC or silica gel column chromatography:

N-Cyclopropyl-3-(4-(2,5-dichlorobenzyl)piperazin-1-yl)-quinoxalin-2-amine (2b). ^1H NMR (400 MHz, CDCl_3) δ ppm 7.72 (t, J = 8.2 Hz, 2H), 7.54 (d, J = 2.2 Hz, 1H), 7.43 (t, J = 7.4 Hz, 1H), 7.32 (br t, J = 7.4 Hz, 1H), 7.27 (d, J = 8.4 Hz, 1H), 7.16 (dd, J = 2.3, 8.5 Hz, 1H), 5.52 (br s, 1H), 3.66 (s, 2H), 3.25 (br s, 4H), 2.92 (br dd, J = 3.3, 6.6 Hz, 1H), 2.69 (br s, 4H), 0.93–0.88 (m, 2H), 0.64–0.53 (m, 2H); ESI-MS calcd for $\text{C}_{22}\text{H}_{23}\text{Cl}_2\text{N}_5$ [$\text{M} + \text{H}$] $^+$ = 427.13, found: 428.0.

N-Cyclopropyl-3-(4-(2,5-dichlorobenzyl)piperazin-1-yl)-7-methylquinoxalin-2-amine (2c). The titled compound was obtained as a mixture of two regioisomers (2:1 ratio). ^1H NMR (400 MHz, CD_3OD) δ ppm 0.87–0.98 (m, 2H), 1.11 (ddt, J = 6.96, 3.45, 1.82, 1.82 Hz, 2H), 2.37–2.46 (m, 3H), 2.65–2.85 (m, 4H), 2.92 (ddt, J = 10.79, 7.22, 3.54, 3.54 Hz, 1H), 3.21–3.29 (m, 4H), 3.73 (s, 2H), 7.17–7.24 (m, 1H), 7.30 (dd, J = 8.53, 2.76 Hz, 1H), 7.37–7.42 (m, 1H), 7.50–7.62 (m, 2H), 7.66–7.81 (m, 1H); ESI-MS calcd for $\text{C}_{23}\text{H}_{25}\text{Cl}_2\text{N}_5$ [$\text{M} + \text{H}$] $^+$ = 441.2, found: 442.0.

N-Cyclopropyl-3-(4-(2,5-dichlorobenzyl)piperazin-1-yl)-7-methoxyquinoxalin-2-amine (2d). ^1H NMR (400 MHz, CD_3OD) δ ppm 0.81–0.90 (m, 2H), 1.04–1.13 (m, 2H), 2.88 (dt, J = 7.09, 3.36 Hz, 1H), 3.58 (br d, J = 2.76 Hz, 8H), 3.94 (s, 3H), 4.56 (s, 2H), 7.15 (dd, J = 9.03, 2.51 Hz, 1H), 7.34 (d, J = 2.76 Hz, 1H), 7.53–7.58 (m, 1H), 7.59–7.63 (m, 1H), 7.72 (d, J = 9.03 Hz, 1H), 7.78 (d, J = 2.26 Hz, 1H); ESI-MS calcd for $\text{C}_{23}\text{H}_{25}\text{Cl}_2\text{N}_5\text{O}$ [$\text{M} + \text{H}$] $^+$ = 457.1, found: 458.0.

N-Cyclopropyl-3-(4-(2,5-dichlorobenzyl)piperazin-1-yl)-7-fluoroquinoxalin-2-amine (2e). ^1H NMR (400 MHz, CD_3OD) δ ppm 0.61–0.68 (m, 2H), 0.90–0.99 (m, 2H), 2.78 (br s, 4H), 2.86 (tt, J = 7.03, 3.64 Hz, 1H), 3.23–3.31 (m, 4H), 3.74 (s, 2H), 7.10 (td, J = 8.66, 2.76 Hz, 1H), 7.24 (dd, J = 8.53, 2.51 Hz, 1H), 7.35 (d, J = 8.53 Hz, 1H), 7.39 (dd, J = 10.29, 2.76 Hz, 1H), 7.56 (d, J = 2.51 Hz, 1H), 7.70 (dd, J = 8.91, 5.90 Hz, 1H); ESI-MS calcd for $\text{C}_{22}\text{H}_{22}\text{Cl}_2\text{FN}_5$ [$\text{M} + \text{H}$] $^+$ = 445.1, found: 446.0.

Synthesis of 2-(Cyclopropylamino)-3-(4-(2,5-dichlorobenzyl)piperazin-1-yl)-N,N-dimethylquinoxaline-6-carboxamide (2h). Step 1: To a solution of methyl 2-(cyclopropylamino)-3-(4-(2,5-dichlorobenzyl)piperazin-1-yl)quinoxaline-6-carboxylate (**2g**, prepared by following the procedures for the synthesis of **2a**) (100 mg, 0.206 mmol, 1.0 equiv) in a mixture of dioxane (3.0 mL) and methanol (1.0 mL) was added an aqueous solution of KOH (2 N, 0.185 mL, 0.370 mmol, 1.8 equiv). The resulting reaction mixture was stirred at rt overnight and then neutralized by the addition of HCl (1.0 N, 0.37 mL). Concentration under reduced pressure gave 2-(cyclopropylamino)-3-(4-(2,5-dichlorobenzyl)piperazin-1-yl)quinoxaline-6-carboxylic acid as a white solid (78% purity), which was used directly in the next step without further purification.

Step 2: A solution of 2-(cyclopropylamino)-3-(4-(2,5-dichlorobenzyl)piperazin-1-yl)quinoxaline-6-carboxylic acid (45 mg, 0.095 mmol, 1.0 equiv) and HATU (36.2 mg, 0.095 mmol, 1.0 equiv) in DMF (1.5 mL) was stirred at rt for 5 min, and then DIPEA (36.9 mg, 0.286 mmol, 3.0 equiv) and dimethylamine hydrochloride (11.7 mg, 0.143 mmol, 1.5 equiv) were added. The resulting solution was stirred at rt for 3 h. The solvent was removed under reduced pressure, and then the residue was purified by silica gel column chromatography (1–5% MeOH in DCM) to give the titled compound **2h** as an

off-white solid (29 mg, 59% yield). ^1H NMR (400 MHz, CD_3OD) δ ppm 0.89–0.96 (m, 2H), 1.06–1.13 (m, 2H), 2.78 (br d, J = 2.76 Hz, 4H), 2.91–2.99 (m, 1H), 3.03 (br s, 3H), 3.12 (br s, 3H), 3.22–3.28 (m, 4H), 3.71–3.77 (m, 2H), 7.21–7.29 (m, 1H), 7.31 (d, J = 2.01 Hz, 1H), 7.34–7.38 (m, 1H), 7.38–7.43 (m, 1H), 7.55 (d, J = 2.51 Hz, 1H), 7.66–7.75 (m, 1H); ESI-MS calcd for $\text{C}_{25}\text{H}_{28}\text{Cl}_2\text{FN}_6\text{O}$ [$\text{M} + \text{H}$] $^+$ = 498.1, found: 499.1.

Synthesis of 3-(Cyclopropylamino)-2-(4-(2,5-dichlorobenzyl)piperazin-1-yl)quinoxaline-6-carbonitrile (2f). Step 1: To a solution of 2,3-dichloroquinoxaline-6-carbonitrile (400 mg, 1.785 mmol, 1.0 equiv) and 1-(2,5-dichlorobenzyl)piperazine hydrogen chloride (8a) (601 mg, 2.14 mmol, 1.2 equiv) in DCM (30 mL) was added DIPEA (0.780 mL, 4.46 mmol, 2.5 equiv) at 20 °C, and the resulting reaction mixture was stirred for 6 h. Water was added, and the reaction was extracted with DCM. The combined organic layers were concentrated, and the residue was purified by silica gel column chromatography (PE/EtOAc = 50:1) to afford 3-chloro-2-(4-(2,5-dichlorobenzyl)piperazin-1-yl)quinoxaline-6-carbonitrile (657 mg, 85% yield) as a yellow solid.

Step 2: A solution of 3-chloro-2-(4-(2,5-dichlorobenzyl)piperazin-1-yl)quinoxaline-6-carbonitrile (30 mg, 0.069 mmol, 1.0 equiv), cyclopropanamine (12 mg, 0.208, 3.0 equiv), and DIPEA (0.030 mL, 0.173 mmol, 2.5 equiv) in dioxane (2.0 mL) in a sealed vial was heated at 100 °C overnight. HPLC purification under acidic conditions afforded the title compound 2f (21 mg, 66%) as a yellow solid. ^1H NMR (400 MHz, methanol- d_4) δ ppm 0.67–0.73 (m, 2H), 0.88–0.97 (m, 2H), 2.88 (tt, J = 7.15, 3.64 Hz, 1H), 3.60 (br s, 8H), 4.58 (s, 2H), 7.55–7.57 (m, 1H), 7.58 (d, J = 1.00 Hz, 1H), 7.60–7.64 (m, 1H), 7.77 (s, 1H), 7.78 (d, J = 5.77 Hz, 1H), 8.04 (d, J = 1.76 Hz, 1H); ESI-MS calcd for $\text{C}_{23}\text{H}_{22}\text{Cl}_2\text{N}_6$ [$\text{M} + \text{H}$] $^+$ = 452.1, found: 453.1.

Synthesis of N-Cyclopropyl-2-(4-(2,5-dichlorobenzyl)piperazin-1-yl)pyrido[3,4-*b*]pyrazin-3-amine (3a). To a solution of 3-chloro-2-[4-[(2,5-dichlorophenyl)methyl]piperazin-1-yl]pyrido[3,4-*b*]pyrazine (13a) (70 mg, 171.3 μmol , 1.0 equiv) and cyclopropanamine (9.8 mg, 171.3 μmol , 1.0 equiv) in dioxane (3.0 mL) was added DIPEA (89.5 μL , 513.8 μmol , 3.0 eq). The resulting mixture was stirred in a 30 mL sealed tube at 100 °C for 30 h. The reaction mixture was evaporated to dryness and purified by prep-HPLC (column: Phenomenex Gemini-NX150 \times 30 mm \times 5 μm ; mobile phase: [water (0.05% $\text{NH}_3\text{H}_2\text{O}$)-ACN]; B%: 60–90%, 7 min) to give N-cyclopropyl-2-[4-[(2,5-dichlorophenyl)methyl]piperazin-1-yl]pyrido[3,4-*b*]pyrazin-3-amine (7.6 mg, 10.2% yield) as a yellow solid. ^1H NMR (400 MHz, CDCl_3) δ ppm 9.02 (s, 1H), 8.38 (br d, J = 6.0 Hz, 1H), 7.61 (d, J = 5.7 Hz, 1H), 7.54 (br s, 1H), 7.31–7.27 (m, 1H), 7.21–7.17 (m, 1H), 5.51 (br s, 1H), 3.69 (s, 2H), 3.51 (br s, 4H), 2.93 (br dd, J = 3.6, 6.7 Hz, 1H), 2.72 (br s, 4H), 1.02–0.91 (m, 2H), 0.68–0.58 (m, 2H); ESI-MS calcd for $\text{C}_{21}\text{H}_{22}\text{Cl}_2\text{N}_6$ [$\text{M} + \text{H}$] $^+$ = 428.13, found: 429.1.

Using similar reaction conditions as described above and utilizing intermediates prepared as described above or commercially available piperazines, the following compounds were synthesized and purified by either HPLC or silica gel column chromatography:

N-Cyclopropyl-2-(4-(2,4-difluorophenoxy)piperidin-1-yl)-7-methylpyrido[3,4-*b*]pyrazin-3-amine (4d). The title compound was prepared in a manner similar to 3a using 10 equiv of cyclopropanamine and 13b at 110 °C to give a dark yellow semisolid (23.8% yield). ^1H NMR (400 MHz, CD_3OD) δ ppm 0.70–0.74 (m, 2H), 0.88–0.90 (m, 2H), 1.93 (dt, J = 6.83, 3.42 Hz, 2H), 2.06–2.15 (m, 2H), 2.71 (s, 3H), 2.90 (dt, J = 7.44, 3.36 Hz, 1H), 3.77–3.80 (m, 2H), 3.99–4.02 (m, 2H), 4.57–4.58 (m, 1H), 6.87–6.89 (m, 1H), 6.99–7.01 (m, 1H), 7.18–7.19 (m, 1H), 7.65 (s, 1H), 8.73 (s, 1H); ESI-MS calcd for $\text{C}_{22}\text{H}_{23}\text{F}_2\text{N}_5\text{O}$ [$\text{M} + \text{H}$] $^+$ = 411.2, found: 412.4.

2-(4-(2,4-Difluorophenoxy)piperidin-1-yl)-N-isopropyl-7-methylpyrido[3,4-*b*]pyrazin-3-amine (4e). The title compound was prepared in a manner similar to 3a using 10 equiv of propan-2-amine and 13b at 110 °C to give a yellow solid (15.6% yield). ^1H NMR (400 MHz, CD_3OD) δ ppm 1.32 (d, J = 6.35 Hz, 6H), 1.93–1.96 (m, 2H), 2.09–2.11 (m, 2H), 2.70 (s, 3H), 3.83–3.84 (m, 2H), 4.05–4.06 (m, 2H), 4.42–4.44 (m, 1H), 6.89 (m, 1H), 7.00–7.02 (m, 1H), 7.19–

7.20 (m, 1H), 7.62 (s, 1H), 8.64 (s, 1H); ESI-MS calcd for $\text{C}_{22}\text{H}_{25}\text{F}_2\text{N}_5\text{O}$ [$\text{M} + \text{H}$] $^+$ = 413.2, found: 414.4.

Synthesis of N-Cyclopropyl-3-(4-(2,5-dichlorobenzyl)piperazin-1-yl)pyrido[3,4-*b*]pyrazin-2-amine (3b). A solution of 3-chloro-N-cyclopropyl-pyrido[3,4-*b*]pyrazin-2-amine (12a) (50 mg, 172.2 μmol , 1.0 equiv), 1-[(2,5-dichlorophenyl)methyl]piperazine (42.2 mg, 172.2 μmol , 1.0 equiv), and DIPEA (90.0 μL , 516.6 μmol , 3.0 equiv) in dioxane (3.0 mL) was stirred at 80 °C for 24 h. The reaction mixture was concentrated under reduced pressure and then purified by prep-HPLC (column: Phenomenex Gemini-NX 150 \times 30 mm \times 5 μm ; mobile phase: [water (0.05% $\text{NH}_3\text{H}_2\text{O}$)-ACN]; B%: 54–84%, 7 min) to give N-cyclopropyl-3-[4-[(2,5-dichlorophenyl)methyl]piperazin-1-yl]pyrido[3,4-*b*]pyrazin-2-amine (17.4 mg, 23.5% yield) as a white solid. ^1H NMR (400 MHz, CDCl_3) δ ppm = 8.98 (s, 1H), 8.46 (d, J = 5.5 Hz, 1H), 7.57–7.46 (m, 2H), 7.28 (d, J = 8.4 Hz, 1H), 7.17 (dd, J = 2.4, 8.6 Hz, 1H), 5.80 (br s, 1H), 3.66 (s, 2H), 3.33–3.19 (m, 4H), 2.96 (dt, J = 3.2, 6.9 Hz, 1H), 2.70 (br s, 4H), 1.01–0.89 (m, 2H), 0.66–0.56 (m, 2H); ESI-MS calcd for $\text{C}_{21}\text{H}_{22}\text{Cl}_2\text{N}_6$ [$\text{M} + \text{H}$] $^+$ = 428.13, found: 429.0.

Using similar reaction conditions as described above and utilizing intermediates prepared as described above or commercially available piperazines, the following compounds were synthesized and purified by either HPLC or silica gel column chromatography:

3-(4-(5-Chloro-2-fluorobenzyl)piperazin-1-yl)-N-cyclopropylpyrido[3,4-*b*]pyrazin-2-amine (3c). The title compound was prepared in a manner similar to 3b using 1-(5-chloro-2-fluorobenzyl)piperazine hydrogen chloride and 12a at 80 °C. ^1H NMR (400 MHz, CD_3OD) δ ppm 0.78–0.86 (m, 2H), 0.93–1.02 (m, 2H), 3.12 (tt, J = 7.40, 3.76 Hz, 1H), 3.45 (br t, J = 4.77 Hz, 4H), 3.74 (br s, 4H), 4.37 (s, 2H), 7.30 (t, J = 9.16 Hz, 1H), 7.56 (ddd, J = 8.78, 4.52, 2.76 Hz, 1H), 7.65 (dd, J = 6.27, 2.76 Hz, 1H), 7.86 (d, J = 6.78 Hz, 1H), 8.41 (dd, J = 6.53, 1.00 Hz, 1H), 8.98 (s, 1H); ESI-MS calcd for $\text{C}_{21}\text{H}_{22}\text{ClFN}_6$ [$\text{M} + \text{H}$] $^+$ = 412.2, found: 413.3.

N-Cyclopropyl-3-(4-(2,5-difluorobenzyl)piperazin-1-yl)pyrido[3,4-*b*]pyrazin-2-amine (3d). The title compound was prepared in a manner similar to 3b using 1-(2,5-difluorobenzyl)piperazine hydrogen chloride and 12a at 80 °C. ^1H NMR (400 MHz, CD_3OD) δ ppm 0.76–0.86 (m, 2H), 0.93–1.02 (m, 2H), 3.08–3.17 (m, 1H), 3.38 (br d, J = 4.02 Hz, 4H), 3.71 (br s, 4H), 4.30 (s, 2H), 7.24–7.32 (m, 2H), 7.37 (ddd, J = 7.28, 5.27, 1.76 Hz, 1H), 7.85 (d, J = 6.53 Hz, 1H), 8.40 (dd, J = 6.52, 0.75 Hz, 1H), 8.96 (s, 1H); ESI-MS calcd for $\text{C}_{21}\text{H}_{22}\text{F}_2\text{N}_6$ [$\text{M} + \text{H}$] $^+$ = 396.2, found: 397.4.

N-Cyclopropyl-3-(4-(2,4-difluorobenzyl)piperazin-1-yl)pyrido[3,4-*b*]pyrazin-2-amine (3e). The title compound was prepared in a manner similar to 3b using 1-(2,4-difluorobenzyl)piperazine hydrogen chloride and 12a at 80 °C (90% yield). ^1H NMR (500 MHz, CDCl_3) δ ppm 0.61–0.65 (m, 2H), 0.94–0.99 (m, 2H), 2.67 (br s, 4H), 2.93–3.00 (m, 1H), 3.26 (t, J = 4.64 Hz, 4H), 3.65 (s, 2H), 6.79–6.85 (m, 1H), 6.86–6.92 (m, 1H), 7.37–7.44 (m, 1H), 7.54 (d, J = 5.37 Hz, 1H), 8.47 (d, J = 5.86 Hz, 1H), 8.98 (s, 1H); ESI-MS calcd for $\text{C}_{21}\text{H}_{22}\text{F}_2\text{N}_6$ [$\text{M} + \text{H}$] $^+$ = 396.2, found: 397.9.

N-Cyclopropyl-3-(4-(2,4-difluorobenzyl)piperazin-1-yl)-7-methylpyrido[3,4-*b*]pyrazin-2-amine (3f). The title compound was prepared in a manner similar to 3b using 1-(2,4-difluorobenzyl)piperazine hydrogen chloride and 12c at 80 °C and obtained as a white solid (22% yield). ^1H NMR (500 MHz, CD_3OD) δ ppm 0.77–0.86 (m, 2H), 0.94–2.04 (m, 2H), 2.75 (s, 3H), 3.13 (tt, J = 7.44, 3.78 Hz, 1H), 3.54 (br s, 8H), 4.48 (s, 2H), 7.12–7.25 (m, 2H), 7.66 (td, J = 8.54, 6.35 Hz, 1H), 7.71 (s, 1H), 8.88 (s, 1H); ESI-MS calcd for $\text{C}_{22}\text{H}_{24}\text{F}_2\text{N}_6$ [$\text{M} + \text{H}$] $^+$ = 410.2, found: 411.0.

3-(4-(2,4-Difluorobenzyl)piperazin-1-yl)-N-isopropylpyrido[3,4-*b*]pyrazin-2-amine (3g). The title compound was prepared in a manner similar to 3b using 1-(2,4-difluorobenzyl)piperazine hydrogen chloride and 12b at 80 °C and obtained as a gray solid (82% yield). ^1H NMR (500 MHz, CD_3OD) δ ppm 1.32 (d, J = 6.35 Hz, 6H), 2.74 (t, J = 4.64 Hz, 4H), 3.36 (br s, 4H), 3.68 (s, 2H), 4.45 (dt, J = 13.06, 6.41 Hz, 1H), 6.90–7.03 (m, 2H), 7.41–7.56 (m, 2H), 8.29 (d, J = 5.37 Hz, 1H), 8.75 (s, 1H); ESI-MS calcd for $\text{C}_{21}\text{H}_{24}\text{F}_2\text{N}_6$ [$\text{M} + \text{H}$] $^+$ = 398.2, found: 399.3.

3-(4-(2,4-Difluorobenzyl)piperazin-1-yl)-N-isopropyl-7-methylpyrido[3,4-b]pyrazin-2-amine (**3h**). The title compound was prepared in a manner similar to **3b** using 1-(2,4-difluorobenzyl)-piperazine hydrogen chloride and **12d** at 80 °C and obtained as a white solid (97% yield). ¹H NMR (500 MHz, CD₃OD) δ ppm 1.35 (d, *J* = 6.83 Hz, 6H), 2.73 (s, 4H), 3.57 (br. s., 6H), 4.48 (s, 2H), 4.66 (quin, *J* = 6.59 Hz, 1H), 7.11–7.24 (m, 2H), 7.61 (s, 1H), 7.68 (td, *J* = 8.54, 6.35 Hz, 1H), 8.83 (s, 1H); ESI-MS calcd for C₂₂H₂₆F₂N₆ [M + H]⁺ = 412.2, found: 413.00.

N-Cyclopropyl-3-(4-(2,4-difluorophenoxy)piperidin-1-yl)-7-methylpyrido[3,4-b]pyrazin-2-amine (**4a**). The title compound was prepared in a manner similar to **3b** using 4-(2,4-difluorophenoxy)-piperidine hydrogen chloride and **12c** at 80 °C and obtained as a light yellow solid (35% yield). ¹H NMR (500 MHz, CD₃OD) δ ppm 1.59–1.64 (m, 2H), 1.64–1.70 (m, 2H), 2.55–2.74 (m, 2H), 2.82–2.98 (m, 2H), 3.45 (s, 3H), 3.82–3.96 (m, 1H), 4.04–4.17 (m, 3H), 4.48 (br. s., 2H), 5.44 (dt, *J* = 7.57, 4.03 Hz, 1H), 7.77–7.91 (m, 1H), 8.03–8.22 (m, 2H), 8.47 (s, 1H), 9.27 (d, *J* = 4.39 Hz, 1H), 9.78 (s, 1H); ESI-MS calcd for C₂₂H₂₃F₂N₅O [M + H]⁺ = 411.2, found: 412.9.

3-(4-(2,4-Difluorophenoxy)piperidin-1-yl)-N-isopropyl-7-methylpyrido[3,4-b]pyrazin-2-amine (**4b**). The title compound was prepared in a manner similar to **3b** using 4-(2,4-difluorophenoxy)-piperidine hydrogen chloride and **12d** at 60 °C and obtained as an off-white solid (43% yield). ¹H NMR (500 MHz, CD₃OD) δ ppm 1.35 (d, *J* = 6.35 Hz, 6H), 1.99 (tdd, *J* = 10.25, 10.25, 7.32, 3.42 Hz, 2H), 2.12–2.22 (m, 2H), 2.71 (s, 3H), 3.45 (ddd, *J* = 13.06, 7.69, 3.66 Hz, 2H), 3.74–3.83 (m, 2H), 4.58 (tt, *J* = 6.83, 3.42 Hz, 1H), 4.64 (quin, *J* = 6.71 Hz, 1H), 6.90 (dddd, *J* = 9.34, 7.87, 3.05, 1.71 Hz, 1H), 7.00 (ddd, *J* = 11.35, 8.66, 2.93 Hz, 1H), 7.20 (td, *J* = 9.28, 5.37 Hz, 1H), 7.56 (s, 1H), 8.73 (s, 1H); ESI-MS calcd for C₂₂H₂₅F₂N₅O [M + H]⁺ = 413.2, found: 414.0.

Synthesis of 3-(4-(2,4-Difluorobenzyl)piperazin-1-yl)-2-(isopropylamino)pyrido[3,4-b]pyrazine-7-carbonitrile (**4c**). A vial containing a mixture of 7-bromo-N-isopropyl-3-(4-(2,4-difluorobenzyl)piperazin-1-yl)pyrido[3,4-b]pyrazin-2-amine (**4g**, prepared in a manner similar to **3b** using 4-(2,4-difluorophenoxy)-piperidine hydrogen chloride and **12e**) (17 mg, 0.035 mmol, 1.0 equiv), Pd₂(dba)₃ (1.581 mg, 1.726 μmol, 0.05 equiv), dicyanozinc (2.433 mg, 0.021 mmol, 0.6 equiv) and 1,1'-bis(diphenylphosphino)ferrocene (dppf) (1.914 mg, 3.4 μmol, 0.1 equiv) in NMP (345 μL) was evacuated and filled with N₂ three times then heated at 120 °C for 2 h. The crude reaction mixture was filtered through a Millipore filter, and purified by HPLC to afford the title compound **4c** as a white solid. ¹H NMR (400 MHz, CD₃OD) δ ppm 1.32 (d, *J* = 6.53 Hz, 6H), 1.29–1.29 (m, 1H), 1.95–2.07 (m, 2H), 2.11–2.24 (m, 2H), 3.35–3.44 (m, 2H), 3.68–3.79 (m, 2H), 4.41–4.51 (m, 1H), 4.55 (td, *J* = 7.15, 3.51 Hz, 1H), 6.83–6.92 (m, 1H), 6.99 (ddd, *J* = 11.32, 8.50, 3.01 Hz, 1H), 7.19 (td, *J* = 9.19, 5.46 Hz, 1H), 7.87 (s, 1H), 8.76 (s, 1H); ESI-MS calcd for C₂₂H₂₃F₂N₇ [M + H]⁺ = 423.2, found: 424.4.

Synthesis of 1-(2-(4-(2,4-Difluorobenzyl)piperazin-1-yl)-3-(isopropylamino)-7,8-dihydropyrido[3,4-b]pyrazin-6(5H)-yl)ethan-1-one (**5a**). To a solution of 2-(4-(2,4-difluorobenzyl)piperazin-1-yl)-N-isopropylpyrido[3,4-b]pyrazin-3-amine (**14**) (0.5 g, 1.255 mmol) in acetone (25 mL) and dioxane (25 mL) was added palladium, 10 wt % on activated carbon (0.053 g, 0.502 mmol) as a slurry in dioxane (3 mL) under nitrogen. Next, acetic anhydride (1.179 mL, 12.55 mmol) was added at 23 °C. The mixture was stirred under hydrogen at 45 °C and 310 kPa for 9.5 h. The reaction mixture was filtered through Celite, rinsed with EtOAc, and concentrated via rotary evaporation. The crude material was dissolved in toluene (5 mL) and purified via medium pressure chromatography using a 10% to 100% gradient eluant of EtOAc in heptane on an NH column. The pure fractions were combined, concentrated via rotary evaporation, and dried *in vacuo* to provide the title compound **5a** (341 mg, 61.1%) as an off-white foam. ¹H NMR (500 MHz, DMSO-*d*₆, mixture of rotamers) δ ppm 1.14–1.19 (m, 6H), 2.08 (s, 1.2H), 2.09 (s, 1.8H), 2.52–2.65 (m, 5H), 2.70 (t, *J* = 5.9 Hz, 1H), 2.98 (br s, 4H), 3.58 (s, 2H), 3.70 (dt, *J* = 12.0, 5.7 Hz,

2H), 4.00–4.15 (m, 1H), 4.40 (s, 0.8H), 4.43 (s, 1.2H), 5.35 (d, *J* = 7.8 Hz, 0.4H), 5.38 (d, *J* = 8.3 Hz, 0.6H) 7.08 (td, *J* = 8.3, 2.4 Hz, 1H), 7.21 (td, *J* = 10.0, 2.4 Hz, 1H), 7.44–7.51 (m, 1H); ESI-MS calcd for C₂₃H₃₀F₂N₆O [M + H]⁺ = 444.2, found: 445.0.

Synthesis of 2-(4-(2,4-Difluorobenzyl)piperazin-1-yl)-N-isopropyl-5,6,7,8-tetrahydropyrido[3,4-b]pyrazin-3-amine (**15**). To a solution of 1-(2-(4-(2,4-difluorobenzyl)piperazin-1-yl)-3-(isopropylamino)-7,8-dihydropyrido[3,4-b]pyrazin-6(5H)-yl)ethanone (**5a**) (0.367 g, 0.826 mmol) in MeOH (4 mL) was added NaOH, 15% solution (2.201 g, 8.26 mmol) at 23 °C. The reaction mixture was stirred at 65 °C for 16 h, cooled to 23 °C, and neutralized with 1 N HCl (9.5 mL) to furnish a suspension. The crude mixture was concentrated via rotary evaporation, and stirred overnight. The resulting solid was filtered, rinsed with water, and dried *in vacuo* to provide the title compound **15** (253 mg, 76%) as a yellow foam. ¹H NMR (500 MHz, DMSO-*d*₆) δ ppm 1.15 (d, *J* = 6.8 Hz, 6H), 2.42 (br s, 1H), 2.51–2.61 (m, 6H), 2.89–3.00 (m, 6H), 3.58 (s, 2H), 3.63 (s, 2H), 4.00–4.10 (m, 1H), 5.15 (d, *J* = 8.3 Hz, 1H), 7.04–7.11 (m, 1H), 7.21 (td, *J* = 10.0, 2.4 Hz, 1H), 7.44–7.52 (m, 1H); ESI-MS calcd for C₂₁H₂₈F₂N₆ [M + H]⁺ = 402.2, found: 403.0.

Synthesis of 1-(2-(4-(2,4-Difluorobenzyl)piperazin-1-yl)-3-(isopropylamino)-7,8-dihydropyrido[3,4-b]pyrazin-6(5H)-yl)propan-1-one (**5b**). To a solution of 2-(4-(2,4-difluorobenzyl)piperazin-1-yl)-N-isopropyl-5,6,7,8-tetrahydropyrido[3,4-b]pyrazin-3-amine (**15**) (50 mg, 0.124 mmol) and DIPEA (0.032 mL, 0.186 mmol) in DCM (1 mL) was added propionic anhydride (0.019 mL, 0.149 mmol) at 0 °C. The reaction mixture was stirred at 0 °C for 1 h, then warmed to 23 °C, and concentrated via rotary evaporation. The resulting crude material was partitioned between EtOAc and water. The organic phase was washed with brine, dried over Na₂SO₄, filtered, rinsed with EtOAc, and concentrated via rotary evaporation. The crude material was dissolved in EtOAc and MeOH, adsorbed on silica gel (0.75 g), and purified via medium pressure silica gel column chromatography using a 20% to 100% gradient of EtOAc in heptane. The pure fractions were combined, concentrated via rotary evaporation, and dried *in vacuo* to provide the title compound **5b** (48 mg, 84% yield) as an off-white foam. ¹H NMR (500 MHz, DMSO-*d*₆, mixture of rotamers) δ ppm 0.94–1.05 (m, 3H), 1.16–1.18 (m, 6H), 2.41 (quin, *J* = 7.8 Hz, 2H), 2.52–2.65 (m, 5H), 2.69 (t, *J* = 5.6 Hz, 1H), 2.98 (br s, 3H), 3.58 (s, 2H), 3.70 (t, *J* = 5.9 Hz, 1.1H), 3.73 (t, *J* = 5.9 Hz, 0.9H), 4.03 (q, *J* = 7.2 Hz, 2H), 4.06–4.15 (m, 1H), 4.42 (br s, 2H), 5.34 (d, *J* = 7.8 Hz, 0.6H), 5.37 (d, *J* = 8.3 Hz, 0.4H), 7.08 (td, *J* = 8.5, 2.4 Hz, 1H), 7.21 (td, *J* = 9.9, 2.7 Hz, 1H), 7.44–7.52 (m, 1 H); ESI-MS calcd for C₂₄H₃₂F₂N₆O [M + H]⁺ = 458.2, found: 459.0.

Synthesis of 2-(4-(2,4-Difluorobenzyl)piperazin-1-yl)-N-isopropyl-6-(methylsulfonyl)-5,6,7,8-tetrahydropyrido[3,4-b]pyrazin-3-amine (**5c**). To a solution of 2-(4-(2,4-difluorobenzyl)piperazin-1-yl)-N-isopropyl-5,6,7,8-tetrahydropyrido[3,4-b]pyrazin-3-amine (50 mg, 0.124 mmol) and DIPEA (0.032 mL, 0.186 mmol) in DCM (1 mL) was added methanesulfonyl chloride (10.6 μL, 0.137 mmol) at 0 °C. The reaction mixture was stirred at 0 °C for 1 h and then concentrated via rotary evaporation. The resulting crude material was partitioned between EtOAc (2 mL) and water (1 mL). The organic phase was washed with brine, dried over Na₂SO₄, filtered, rinsed with EtOAc, and concentrated via rotary evaporation. The crude material was dissolved in EtOAc and MeOH, adsorbed on silica gel (0.75 g), and purified via medium pressure silica gel column chromatography using a gradient eluant of 50% to 100% EtOAc in heptane. The pure fractions were combined, concentrated via rotary evaporation, and dried *in vacuo* to provide the title compound **5c** (50.6 mg, 85%) as an off-white solid. ¹H NMR (500 MHz, DMSO-*d*₆) δ ppm 1.12–1.19 (m, 6H), 2.53–2.61 (m, 4H), 2.74 (t, *J* = 5.9 Hz, 2H), 2.97 (s, 3H), 3.00 (d, *J* = 7.3 Hz, 4H), 3.44–3.48 (m, 1H), 3.59 (s, 2H), 4.02–4.10 (m, 1H), 4.16 (s, 2H), 5.41 (d, *J* = 7.8 Hz, 1H), 7.08 (td, *J* = 8.4, 2.2 Hz, 1H), 7.22 (td, *J* = 9.9, 2.7 Hz, 1H), 7.44–7.54 (m, 1H); ESI-MS calcd for C₂₂H₃₀F₂N₆O₂S [M + H]⁺ = 480.2, found: 480.9.

Substrates **16a,b** were prepared under the reaction conditions similar to **3b** (Scheme 2) through double S_NAr reactions on **11a** with isopropylamine (or cyclopropylamine) and 4-(2,4-difluorophenoxy)-piperidine sequentially. Substrates **17a,b** were prepared under the

reaction conditions similar to **3a** through double SNAr reactions on **11a** with 4-(2,4-difluorophenoxy)piperidine and isopropylamine (or cyclopropylamine) sequentially.

Synthesis of 2-(4-(2,4-Difluorophenoxy)piperidin-1-yl)-N-isopropyl-5,6,7,8-tetrahydropyrido[3,4-*b*]pyrazin-3-amine (6c). Step 1: To a yellow-orange suspension of 2-(4-(2,4-difluorophenoxy)piperidin-1-yl)-N-isopropylpyrido[3,4-*b*]pyrazin-3-amine **17a** (5.1 g, 12.77 mmol) in MeCN (63.8 mL) was added benzyl bromide (2.184 g, 12.77 mmol) over 1 min at rt. The mixture was stirred at 80 °C for 4 h to furnish a red-brown solution, cooled to 23 °C, and then concentrated via rotary evaporation to provide 6-benzyl-2-(4-(2,4-difluorophenoxy)piperidin-1-yl)-3-(isopropylamino)pyrido[3,4-*b*]pyrazin-6-ium bromide (7.30 g) as a red-brown solid, which was used directly in the next step without further purification.

Step 2: To a solution of 6-benzyl-2-(4-(2,4-difluorophenoxy)piperidin-1-yl)-3-(isopropylamino)pyrido[3,4-*b*]pyrazin-6-ium bromide (7.2 g, 12.62 mmol) in DCM (126 mL) was added NaBH(OAc)₃ (16.05 g, 76 mmol) in one portion at rt. The resulting solution was stirred at rt for 3 days. The solvent was removed under reduced pressure, and EtOAc (200 mL) was added to redissolve the residue. Saturated NaHCO₃ (150 mL) was added, and the mixture was vigorously stirred for 30 min. The organic layer was washed with water (50 mL) and brine (50 mL), and dried with anhydrous Na₂SO₄ overnight. Removal of the solvent gave 6-benzyl-2-(4-(2,4-difluorophenoxy)piperidin-1-yl)-N-isopropyl-5,6,7,8-tetrahydropyrido[3,4-*b*]pyrazin-3-amine (6.43 g) as a yellow solid, which was used without further purification. ESI-MS calcd for C₂₈H₃₃F₂N₅O [M + H]⁺ = 493.3, found: 494.1.

Step 3: A mixture of 6-benzyl-2-(4-(2,4-difluorophenoxy)piperidin-1-yl)-N-isopropyl-5,6,7,8-tetrahydropyrido[3,4-*b*]pyrazin-3-amine (6.43 g, 13.03 mmol) and 10% Pd/C (640 mg) in MeOH (86 mL) under H₂ in a balloon was stirred at rt overnight. Removal of the solvent gave 2-(4-(2,4-difluorophenoxy)piperidin-1-yl)-N-isopropyl-5,6,7,8-tetrahydropyrido[3,4-*b*]pyrazin-3-amine (**6c**) (4.4 g, 84%) as a yellow oil. ¹H NMR (400 MHz, CD₃OD) δ ppm 1.24 (d, *J* = 6.4 Hz, 6H), 1.89–1.99 (m, 2H), 2.09–2.17 (m, 2H), 2.74 (t, *J* = 5.9 Hz, 2H), 2.95 (ddd, *J* = 12.3, 8.7, 3.4 Hz, 2H), 3.11 (t, *J* = 6.1 Hz, 2H), 3.82 (s, 2H), 4.14 (septet, *J* = 6.4 Hz, 1H), 4.46 (tt, *J* = 7.7, 3.5 Hz, 1H), 6.85–6.92 (m, 1H), 6.99 (ddd, *J* = 11.4, 8.4, 3.2 Hz, 1H), 7.18 (td, *J* = 9.3, 5.4 Hz, 1H); ESI-MS calcd for C₂₁H₂₇F₂N₅O [M + H]⁺ = 403.2, found: 404.0.

Compounds **18a**, **18b**, and **19a** were prepared in a reaction sequence similar to the synthesis of **6c**, starting with **16a**, **16b**, and **17b**, respectively.

Preparation of 1-(3-(4-(2,4-Difluorophenoxy)piperidin-1-yl)-2-(isopropylamino)-7,8-dihydropyrido[3,4-*b*]pyrazin-6(5H)-yl)-ethanone (6a). Acetic anhydride (5 μL, 0.058 mmol) was added to a solution of 3-(4-(2,4-difluorophenoxy)piperidin-1-yl)-N-isopropyl-5,6,7,8-tetrahydropyrido[3,4-*b*]pyrazin-2-amine TFA salt (**18a**) (15.1 mg, 0.029 mmol) and pyridine (7 μL, 0.088 mmol) in DCM (290 μL) at rt. After being stirred for 1 h, the mixture was purified by HPLC to afford the title compound **6a** as its TFA salt (12.7 mg, 78%) as a yellow film. ¹H NMR (400 MHz, CD₃OD, mixture of two rotamers) δ ppm 1.33 (d, *J* = 6.6 Hz, 6H), 1.91–2.02 (m, 2H), 2.09–2.18 (m, 2H), 2.19 (s, 1.4H), 2.21 (s, 1.6H), 2.77–2.83 (m, 0.9H), 2.88–2.94 (m, 1.1H), 3.12 (td, *J* = 8.5, 4.0 Hz, 2H), 3.43–3.51 (m, 2H), 3.80–3.85 (m, 1.1H), 3.86–3.91 (m, 0.9H), 4.10–4.18 (m, 1H), 4.47–4.54 (m, 1H), 4.55 (br s, 2H), 6.85–6.92 (m, 1H), 6.99 (ddd, *J* = 11.4, 8.6, 3.0 Hz, 1H), 7.18 (td, *J* = 9.2, 5.6 Hz, 1H); ESI-MS calcd for C₂₃H₂₇F₂N₅O₂ [M + H]⁺ = 445.2, found: 446.4.

Preparation of 1-(2-(Cyclopropylamino)-3-(4-(2,4-difluorophenoxy)piperidin-1-yl)-7,8-dihydropyrido[3,4-*b*]pyrazin-6(5H)-yl)ethanone (6b). To a solution of N-cyclopropyl-3-(4-(2,4-difluorophenoxy)piperidin-1-yl)-5,6,7,8-tetrahydropyrido[3,4-*b*]pyrazin-2-amine (**18b**) (1.76 g, 4.38 mmol) in DCM (50 mL) at 0 °C was added acetyl chloride (0.467 mL, 6.58 mmol) and DIPEA (2.291 mL, 13.15 mmol) dropwise. The resulting solution was stirred at rt for 10 min and then concentrated under reduced pressure. The residue was purified by HPLC to give the title compound **6b** (699 mg, 36%) as a white solid. Melting point: 106.8 °C. ¹H NMR (500 MHz,

CDCl₃) δ ppm 0.66–0.75 (m, 2 H) 1.03–1.13 (m, 2 H) 1.94–2.03 (m, 2 H) 2.08–2.15 (m, 2 H) 2.23–2.28 (m, 3 H) 2.96–3.14 (m, 5 H) 3.38–3.47 (m, 2 H) 3.75–3.83 (m, 1 H) 3.90–3.97 (m, 1 H) 4.38–4.45 (m, 1 H) 4.51–4.56 (m, 1 H) 4.66–4.70 (m, 1 H) 6.78–6.85 (m, 1 H) 6.86–6.92 (m, 1 H) 6.97–7.04 (m, 1 H); ESI-MS calcd for C₂₃H₂₇F₂N₅O₂ [M + H]⁺ = 443.2, found: 444.4.

Preparation of 2-(4-(2,4-Difluorophenoxy)piperidin-1-yl)-N-isopropyl-6-methyl-5,6,7,8-tetrahydropyrido[3,4-*b*]pyrazin-3-amine (6d). Sodium triacetoxyhydroborate (9.9 mg, 0.047 mmol) was added to a solution of DIPEA (8 μL, 0.047 mmol), 2-(4-(2,4-difluorophenoxy)piperidin-1-yl)-N-isopropyl-5,6,7,8-tetrahydropyrido[3,4-*b*]pyrazin-3-amine (**6c**) (12.1 mg, 0.023 mmol) and formaldehyde (2 μL, 0.023 mmol) in MeOH (230 μL) at rt. After 30 min, the mixture was purified by HPLC to afford the title compound **6d** as a TFA salt (8.9 mg, 71.6%) as a yellow film. ¹H NMR (400 MHz, methanol-*d*₄) δ ppm 1.24 (d, *J* = 6.3 Hz, 6H), 1.90–2.00 (m, 2H), 2.08–2.17 (m, 2H), 2.95–3.06 (m, 3H), 3.12 (br s, 4H), 3.35–3.53 (m, 3H), 3.76 (br s, 1H), 4.15 (dt, *J* = 13.1, 6.5, 6.5 Hz, 1H), 4.19–4.38 (m, 2H), 4.48 (tt, *J* = 7.3, 3.7 Hz, 1H), 6.85–6.92 (m, 1H), 6.99 (ddd, *J* = 11.4, 8.5, 3.0 Hz, 1H), 7.17 (td, *J* = 9.2, 5.6 Hz, 1H); ESI-MS calcd for C₂₂H₂₅F₂N₅O [M + H]⁺ = 417.2, found: 418.3.

Preparation of 2-(4-(2,4-Difluorophenoxy)piperidin-1-yl)-N-isopropyl-6-(methylsulfonyl)-5,6,7,8-tetrahydropyrido[3,4-*b*]pyrazin-3-amine (6e). In a 50 mL round-bottomed flask equipped with a stir bar, a solution of 2-(4-(2,4-difluorophenoxy)piperidin-1-yl)-N-isopropyl-5,6,7,8-tetrahydropyrido[3,4-*b*]pyrazin-3-amine TFA salt (**6c**) (735.3 mg, 1.421 mmol) in DCM (14.2 mL) at 0 °C was treated with triethylamine (0.594 mL, 4.26 mmol), followed by addition of methanesulfonyl chloride (0.221 mL, 2.84 mmol). The reaction mixture was stirred at 0 °C for 1 h. The reaction mixture was concentrated under reduced pressure. The residue was purified by HPLC to give the title compound **6e** as an off-white solid (229.6 mg, 33.6%). ¹H NMR (500 MHz, DMSO-*d*₆) δ ppm 1.18 (d, *J* = 6.3 Hz, 6H), 1.88 (m, 2H), 2.07 (m, 2H), 2.75 (t, *J* = 5.9 Hz, 2H), 2.89 (m, 2H), 2.97 (s, 3H), 3.29 (m, 2H), 3.45 (t, *J* = 5.9 Hz, 2H), 4.09 (m, 1H), 4.16 (s, 2H), 4.52 (tt, *J* = 8.1, 3.9 Hz, 1H), 5.57 (d, *J* = 8.3 Hz, 1H), 7.01 (m, 1H), 7.30 (m, 2H); ESI-MS calcd for C₂₂H₂₉F₂N₅O₃S [M + H]⁺ = 481.2, found: 481.90.

Preparation of Methyl 2-(4-(2,4-difluorophenoxy)piperidin-1-yl)-3-(isopropylamino)-7,8-dihydropyrido[3,4-*b*]pyrazine-6(5H)-carboxylate (6f). To a solution of 2-(4-(2,4-difluorophenoxy)piperidin-1-yl)-N-isopropyl-5,6,7,8-tetrahydropyrido[3,4-*b*]pyrazin-3-amine (**6c**) (45.6 mg, 0.113 mmol) and triethylamine (0.039 mL, 0.283 mmol) in DCM (0.75 mL) was added methyl carbonochloridate (0.013 mL, 0.170 mmol) at 0 °C. The reaction mixture was stirred at 0 °C for 1 h, warmed to 23 °C, and concentrated under reduced pressure. The resulting crude material was partitioned between EtOAc and H₂O. The organic phase was washed with brine, dried over Na₂SO₄, filtered, rinsed with EtOAc, and concentrated under reduced pressure. The crude material was purified by silica gel column chromatography (2% to 80% gradient eluant of EtOAc in heptane) to provide the title compound **4i** (48.7 mg, 93%) as a white foam. ¹H NMR (500 MHz, DMSO-*d*₆) δ ppm 1.17–1.19 (m, 6H), 1.80–1.94 (m, 2H), 2.06 (ddd, *J* = 9.5, 5.9, 3.2 Hz, 2H), 2.64 (t, *J* = 5.9 Hz, 2H), 2.82–2.94 (m, 2H), 3.19–3.31 (m, 2H), 3.64 (s, 3H), 3.64–3.69 (m, 2H), 4.07–4.17 (m, 1H), 4.35 (br s, 2H), 4.51 (tt, *J* = 8.1, 3.9 Hz, 1H), 5.53 (d, *J* = 8.3 Hz, 1H), 7.01 (dddd, *J* = 9.3, 8.1, 3.2, 1.5 Hz, 1H), 7.26–7.35 (m, 2H); ESI-MS calcd for C₂₃H₂₉F₂N₅O₃ [M + H]⁺ = 461.2, found: 461.9.

Preparation of 1-(3-(cyclopropylamino)-2-(4-(2,4-difluorophenoxy)piperidin-1-yl)-7,8-dihydropyrido[3,4-*b*]pyrazin-6(5H)-yl)ethanone (6g) is similar to the synthesis of compound **6a** starting with N-cyclopropyl-2-(4-(2,4-difluorophenoxy)piperidin-1-yl)-5,6,7,8-tetrahydropyrido[3,4-*b*]pyrazin-3-amine (**19a**). ¹H NMR (500 MHz, CDCl₃) δ ppm 0.46–0.56 (m, 2H) 0.78–0.87 (m, 2H) 1.87–1.96 (m, 2H) 2.05–2.14 (m, 2H) 2.18–2.22 (m, 3H) 2.72–2.94 (m, 5H) 3.27–3.37 (m, 2H) 3.70–3.77 (m, 1H) 3.86–3.92 (m, 1H) 4.28–4.36 (m, 1H) 4.56 (s, 1H) 4.70 (s, 1H) 5.05–5.15 (m,

1H) 6.76–6.82 (m, 1H) 6.84–6.90 (m, 1H) 6.96–7.03 (m, 1H); ESI-MS calcd for $C_{23}H_{27}F_2N_3O_2$ $[M + H]^+ = 443.2$, found: 444.4.

2-(4-(2,4-Difluorophenoxy)piperidin-1-yl)-N-isopropyl-6-(methylsulfonyl)-5,6,7,8-tetrahydropyrido[3,4-*b*]pyrazin-3-amine (**6h**) was prepared in a manner similar to the synthesis of **6a** starting with **6c** and acetic anhydride. 1H NMR (400 MHz, CD_3OD , mixture of two rotamers) δ ppm 1.23 (d, $J = 6.6$ Hz, 3.3H), 1.24 (d, $J = 6.6$ Hz, 2.7H), 1.93 (m, 2H), 2.11 (m, 2H), 2.18 (s, 1.3H), 2.20 (s, 1.7H), 2.71 (t, $J = 6.1$ Hz, 0.9H), 2.80 (t, $J = 6.1$ Hz, 1.1H), 2.95 (m, 2H), 3.34 (m, 2H), 3.79 (t, $J = 5.9$ Hz, 1.1H), 3.84 (t, $J = 6.1$ Hz, 0.9H), 4.15 (m, 1H), 4.44 (t, $J = 7.5$, 3.7 Hz, 1H), 4.53 (s, 0.9H), 4.54 (s, 1.1H), 6.86 (m, 1H), 6.97 (ddd, $J = 11.2$, 8.5, 3.2 Hz, 1H), 7.16 (td, $J = 9.2$, 5.6 Hz, 1H); ESI-MS calcd for $C_{23}H_{29}F_2N_3O_2$ $[M + H]^+ = 445.2$, found: 446.0.

Preparation of (R)-1-(2-(4-(2,4-difluorophenoxy)piperidin-1-yl)-3-((tetrahydrofuran-3-yl)amino)-7,8-dihydropyrido[3,4-*b*]pyrazin-6(5H)-yl)ethan-1-one (**6i**) is similar to the synthesis of compound **6a** starting with (R)-2-(4-(2,4-difluorophenoxy)piperidin-1-yl)-N-(tetrahydrofuran-3-yl)pyrido[3,4-*b*]pyrazin-3-amine (**17c**). 1H NMR (500 MHz, DMSO- d_6 , mixture of two rotamers) δ ppm 1.83–2.00 (m, 3H), 2.06 (dd, $J = 6.83$, 3.42 Hz, 2H), 2.09 (d, $J = 3.42$ Hz, 3H), 2.13–2.23 (m, 1H), 2.60 (t, $J = 5.86$ Hz, 1H), 2.72 (t, $J = 5.86$ Hz, 1H), 2.84–2.95 (m, 2H), 3.29 (br. s., 1H), 3.56 (dt, $J = 8.79$, 5.37 Hz, 1H), 3.68–3.75 (m, 3H), 3.82–3.88 (m, 1H), 3.90 (ddd, $J = 8.79$, 6.10, 2.68 Hz, 1H), 4.35–4.41 (m, 1H), 4.42 (s, 1H), 4.45 (s, 1H), 4.51 (tt, $J = 8.12$, 3.84 Hz, 1H), 5.90 (dd, $J = 13.42$, 6.10 Hz, 1H), 7.01 (dddd, $J = 9.28$, 8.05, 2.93, 1.71 Hz, 1H), 7.23–7.35 (m, 2H); SI-MS calcd for $C_{34}H_{39}F_2N_5O_3$ $[M + H]^+ = 473.2$, found: 474.3.

GPR6 cAMP TR-FRET Assay. Cell-based GPR6 cAMP TR-FRET assays were used to quantify GPR6 receptor-dependent modulation of the cAMP level in CHO-K1 cells. The unusually high level of apparent constitutive activity of GPR6 in heterologous expression systems provided the opportunity to measure inhibition of GPR6 without agonist stimulation. T-REX-CHO-K1 cells (Invitrogen, USA) stably expressing tetracycline inducible human GPR6 were cultured in growth media (F12K medium [Gibco, Life Technologies], containing 10% tetracycline free fetal bovine serum FBS [HyClone, Fisher Scientific], 1% penicillin/streptomycin, and 200 μ g/mL Hygromycin B). To induce GPR6 expression, cells were dissociated and plated in induction media (growth media plus 2.0 μ g/mL doxycycline [Sigma D9891]) at a density of 250–500 cells per well in half area white solid bottom 96-well plates (Costar) and incubated (37 $^{\circ}C$, 5% CO_2) for 20 h. Following incubation, media was removed, and cells were washed with 50 μ L of Krebs Ringer's buffer (Sigma K4002). Source plates containing test compounds suspended in DMSO were diluted in Krebs Ringer's buffer containing 0.5% fatty acid free BSA. Cells were incubated with compound for 45 min at 37 $^{\circ}C$ and 5% CO_2 , followed by Eu-cAMP tracer for 10 min and ULight-anti-cAMP antibody for 1 h at room temperature (PerkinElmer Lance Ultra cAMP assay (TRF0264)). TR-FRET signal was detected on an Envision plate reader (PerkinElmer). IC_{50} curves were generated with a four-parameter logistic equation using GraphPad Prism 5.03.

GPR6 Radioligand Binding Assay. RL-338 was synthesized in the chemistry laboratories of Envoy Therapeutics, Inc., FL. In vitro pharmacological profiling showed that RL-338 is a potent and highly selective GPR6 IAG, inhibiting GPR6 cAMP signaling in TR-FRET assays with a $EC_{50} = 16$ nM and >100 fold selectivity against GPR3 and GPR12 (unpublished). RL-338 was radiolabeled with three tritium atoms by the Quotient Bioresearch (Cardiff, UK) and validated using standard in vitro pharmacology methods (Supporting Information). To study the binding characteristics of GPR6 IAG compounds, a competition binding assay using a filtration-based format was developed featuring membranes prepared from T-REX-CHO-GPR6 cells expressing human GPR6 cDNA driven by a doxycycline inducible promoter. First, assay-ready 96-well plates (651201, Greiner, USA) containing serial dilutions of test compounds (1 μ L of test ligand/well) were prepared in DMSO using liquid handlers (5 μ M, final assay top concentration). A total of 39 μ L of assay buffer was added, and plates were mixed on a plate shaker for 10 min. Next, 40 μ L of radioligand 3H -RL-338 prepared in assay buffer

(50 mM Tris, pH 7.4, 50 mM NaCl, 6 mM $MgCl_2$, fatty acid free 0.1% BSA, proteinase inhibitor cocktail, Sigma USA) was added per well (2.4 nM final assay concentration). Binding reactions were initiated by adding 40 μ L of total membranes obtained from cells expressing human GPR6 receptors. Membranes were prepared in assay buffer (50 mM Tris, pH 7.4, 50 mM NaCl, 6 mM $MgCl_2$, fatty acid free 0.1% BSA, 1 \times proteinase inhibitor cocktail, Sigma USA) and added per well to 15 μ g/well final assay concentration. Plates were sealed, mixed for 30 s at 300 rpm, and incubated for 2 h at room temperature. Reactions were filtered through filtermates (1450-421, filtermate A, PerkinElmer, USA), and washed five times for 5 s with 4 $^{\circ}C$ cold 50 mM Tris, pH 7.4, 50 mM NaCl, 6 mM $MgCl_2$, fatty acid free 0.1% BSA using a Tomtec Harvester 96 instrument. Filters were dried in the microwave, scintillant sheet (1450-411, PerkinElmer, USA) melted on them and heat-sealed before CPM/wells were quantified in a Microbeta Trilux instrument (PerkinElmer, USA). Before use, filtermates were presoaked in 0.5% polyethylenimine solution for 3 h with gentle shaking, followed by air drying overnight.

The same protocol was used for saturation binding assays to determine radioligand 3H -RL-338 affinity to GPR6. Different concentrations of radioligand 3H -RL-338 ranging from 32 nM (high concentration) to 0.015 nM (low concentration) with 1:2 dilution steps were tested to generate saturation curves and obtain the equilibrium dissociation constant K_d . Nonspecific background binding of 3H -RL-338 was determined using 10 nM of an unlabeled structurally diverse potent and selective GPR6 inverse agonists (data not shown). IC_{50} and K_d values were calculated using nonlinear regression analysis in Prism (GraphPad, USA). Saturation curves were fitted to the Prism equation: one site - fit total and nonspecific binding without constraints. Dose-response curves were fitted to the four-parameter variable slope model without constraints in Prism to obtain IC_{50} 's. K_i values were calculated using the Cheng–Prusoff equation (Cheng and Prusoff, 1973). CVN424 and other GPR6 IAG fully displaced 3H -RL-338 from GPR6 and displayed binding properties that were consistent with a single binding site. Radioligand 3H -RL-338 demonstrated high affinity for human GPR6 receptors stably expressed in T-REX-CHO-GPR6 cells ($K_d = 2.4$ nM or 5 nM dependent on synthesized radioligand batch) in saturation binding assays.

Haloperidol-Induced Catalepsy. Haloperidol-induced catalepsy in rodents is caused by blocking activity of striatal dopamine D2 receptors, resulting in elevated cAMP and overactivity of the indirect pathway of the striatum and decreased movement. Compounds **3e** was tested for reversal of haloperidol-induced catalepsy in male wild-type Sprague-Dawley rats (source: Harlan, Frederick (MD) USA), male C57BL/6N (source: wild-type mice (source: Jackson Laboratories, ME, USA) and GPR6 knock out mice using the bar test.²² The cataleptic state was induced by the subcutaneous administration of the dopamine receptor antagonist haloperidol (0.3 mg/kg, sc rats and 1 mg/kg i.p. mice), 90 min before testing the animals. Front paws were placed on a horizontal metal bar raised 2' (mice) or 6' (rats) above a Plexiglas platform and time was recorded for up to 60 s. The test ended when the animal's front paws returned to the platform or after 60 s. The test was repeated three times, and the average of the trials reported. Cataleptic animals treated with haloperidol will hold to the bar without moving for several minutes. Efficacy of compound **3e** to reverse haloperidol-induced catalepsy was tested 120 min post injection. The A2a antagonist KW6002 (Istradefylline) was dosed at 0.6 mg/kg i.p. as a positive control.

Bilateral 6-OHDA-Lesioned Parkinson's Disease Rat Model. Bilateral striatal 6-OHDA lesion in rats trigger degeneration of dopaminergic neurons, striatal dopamine depletion and show motor deficits, which mimics aspects of human PD pathology and symptomatology. Early lead compound **6h** was tested for anti-parkinsonian efficacy in this model, administered as monotherapy (1 mg/kg, p.o.). Thirty minutes prior to surgery, animals (female Sprague-Dawley rats, Charles River Laboratories, Wilmington, MA USA) received pargyline (5 mg/kg; i.p.) and desipramine (10 mg/kg; i.p.) to optimize subsequent 6-hydroxydopamine (6-OHDA) availability and increase specificity for toxicity to dopaminergic

neurons. Rats received bilateral injections of 6-OHDA (20 μ g in 3 μ L; 0.5 μ L/min) into the striatum at coordinates AP: ML: DV, 1, \pm 3, \pm 5 mm relative to Bregma to introduce lesion. Open field activity of animals was recorded pre- and 28 days postsurgery for 3 h. Bilateral lesions induced a significant reduction in activity (40%) compared to prelesion. In addition, there was a 32% reduction of dopamine transporter expression in the striatum (not shown). Directly after dosing compound **6h** locomotor activity (defined as beam broken on the lower level) was assessed in open field arenas equipped with automatic activity monitors (Linton Instrumentation, U.K.).

■ ASSOCIATED CONTENT

■ Supporting Information

The Supporting Information is available free of charge at <https://pubs.acs.org/doi/10.1021/acs.jmedchem.0c02081>.

Materials and Methods; preparation of key intermediates; characterization of lead compounds: **1**, **3e**, and **6h**; original pharmacology data for compound **3e** and lead compound **6h**; structure and validation data of radioligand [3 H]-RL338; reference compound for cAMP TR-FRET assays: structure and in vitro pharmacology; compound **3e** in vitro pharmacology graphs (PDF)

Molecular formula strings (CSV)

■ AUTHOR INFORMATION

Corresponding Authors

Huikai Sun – Takeda California, San Diego, California 92121, United States; orcid.org/0000-0002-4593-1306; Phone: 619-930-8349; Email: Huikai.sun@takeda.com

Holger Monenschein – Takeda California, San Diego, California 92121, United States; Email: holger.m@takeda.com

Authors

Hans H. Schiffer – Takeda California, San Diego, California 92121, United States

Holly A. Reichard – Takeda California, San Diego, California 92121, United States

Shota Kikuchi – Takeda California, San Diego, California 92121, United States

Maria Hopkins – Takeda California, San Diego, California 92121, United States

Todd K. Macklin – Takeda California, San Diego, California 92121, United States

Stephen Hitchcock – Takeda California, San Diego, California 92121, United States

Mark Adams – Takeda California, San Diego, California 92121, United States

Jason Green – Takeda California, San Diego, California 92121, United States

Jason Brown – Takeda California, San Diego, California 92121, United States

Sean T. Murphy – Takeda California, San Diego, California 92121, United States

Nidhi Kaushal – Takeda California, San Diego, California 92121, United States

Deanna R. Colia – Takeda California, San Diego, California 92121, United States

Steve Moore – Takeda California, San Diego, California 92121, United States

William J. Ray – Takeda California, San Diego, California 92121, United States

Mark Beresford Lewis Carlton – Cerevance Ltd, Cambridge, U.K.

Nicola L. Brice – Cerevance Ltd, Cambridge, U.K.

Complete contact information is available at: <https://pubs.acs.org/doi/10.1021/acs.jmedchem.0c02081>

Notes

The authors declare no competing financial interest.

■ ACKNOWLEDGMENTS

We thank the following individuals for their contributions: Ron Chen, Padma Manam, Yang Song, and Paddi Ekhlassi for analytical chemistry and formulation support, Ron Steigerwalt for drug safety expertise, and our process chemistry colleagues Wolfgang Notz, Chunrong Ma, and Dave Provencal.

■ ABBREVIATIONS USED

cAMP, cyclic adenosine monophosphate; DCM, dichloromethane; DMF, *N,N*-dimethylformamide; HPLC, high-performance liquid chromatography; Hz, hertz; LC-MS, liquid chromatography–mass spectrometry; MW, microwave; NMR, nuclear magnetic resonance; rt, room temperature; TEA, triethylamine; TFA, trifluoroacetic acid; THF, tetrahydrofuran

■ REFERENCES

- (1) Poewe, W.; Seppi, K.; Tanner, C. M.; Halliday, G. M.; Brundin, P.; Volkman, J.; Schrag, A. E.; Lang, A. E. Parkinson disease. *Nat. Rev. Dis. Primers* **2017**, *3*, 17013.
- (2) Poewe, W.; Mahlknecht, P. The clinical progression of Parkinson's disease. *Parkinsonism Relat. Disord.* **2009**, *15* (Suppl4), S28–32.
- (3) Poewe, W.; Mahlknecht, P.; Jankovic, J. Emerging therapies for Parkinson's disease. *Curr. Opin. Neurol.* **2012**, *25* (4), 448–459.
- (4) Fearnley, J. M.; Lees, A. J. Ageing and Parkinson's disease: substantia nigra regional selectivity. *Brain* **1991**, *114* (5), 2283–2301.
- (5) Dickson, D. W.; Braak, H.; Duda, J. E.; Duyckaerts, C.; Gasser, T.; Halliday, G. M.; Hardy, J.; Leverenz, J. B.; Del Tredici, K.; Wszolek, Z. K.; Litvan, I. Neuropathological assessment of Parkinson's disease: refining the diagnostic criteria. *Lancet Neurol.* **2009**, *8* (12), 1150–1157.
- (6) McGregor, M. M.; Nelson, A. B. Circuit Mechanisms of Parkinson's Disease. *Neuron* **2019**, *101* (6), 1042–1056.
- (7) Salat, D.; Tolosa, E. Levodopa in the treatment of Parkinson's disease: current status and new developments. *J. Parkinson's Dis.* **2013**, *3* (3), 255–269.
- (8) Tambasco, N.; Romoli, M.; Calabresi, P. Levodopa in Parkinson's Disease: Current Status and Future Developments. *Curr. Neuropharmacol.* **2018**, *16* (8), 1239–1252.
- (9) Tambasco, N.; Belcastro, V.; Gallina, A.; Castrioto, A.; Calabresi, P.; Rossi, A. Levodopa-induced breathing, cognitive and behavioral changes in Parkinson's disease. *J. Neurol.* **2011**, *258* (12), 2296–2299.
- (10) Fabbrini, G.; Brotchie, J. M.; Grandas, F.; Nomoto, M.; Goetz, C. G. Levodopa-induced dyskinesias. *Mov. Disord.* **2007**, *22* (10), 1379–1389.
- (11) Waters, C. Catechol-O-methyltransferase (COMT) inhibitors in Parkinson's disease. *J. Am. Geriatr. Soc.* **2000**, *48* (6), 692–698.
- (12) Riederer, P.; Muller, T. Monoamine oxidase-B inhibitors in the treatment of Parkinson's disease: clinical-pharmacological aspects. *J. Neural Transm. (Vienna)* **2018**, *125* (11), 1751–1757.
- (13) Blandini, F.; Armentero, M. T. Dopamine receptor agonists for Parkinson's disease. *Expert Opin. Invest. Drugs* **2014**, *23* (3), 387–410.
- (14) Connolly, B. S.; Lang, A. E. Pharmacological treatment of Parkinson disease: a review. *JAMA* **2014**, *311* (16), 1670–1683.
- (15) Fox, S. H. Non-dopaminergic treatments for motor control in Parkinson's disease. *Drugs* **2013**, *73* (13), 1405–1415.

- (16) Sahoo, A. K.; Gupta, D.; Singh, A. Istradefylline: a novel drug for 'off' episodes in Parkinson's disease. *Drugs & Therapy Perspectives* **2020**, *36*, 208–212.
- (17) Deuschl, G.; Agid, Y. Subthalamic neurostimulation for Parkinson's disease with early fluctuations: balancing the risks and benefits. *Lancet Neurol.* **2013**, *12* (10), 1025–1034.
- (18) Uhlenbrock, K.; Gassenhuber, H.; Kostenis, E. Sphingosine 1-phosphate is a ligand of the human gpr3, gpr6 and gpr12 family of constitutively active G protein-coupled receptors. *Cell. Signalling* **2002**, *14* (11), 941–953.
- (19) Ignatov, A.; Lintzel, J.; Kreienkamp, H. J.; Schaller, H. C. Sphingosine-1-phosphate is a high-affinity ligand for the G protein-coupled receptor GPR6 from mouse and induces intracellular Ca²⁺ release by activating the sphingosine-kinase pathway. *Biochem. Biophys. Res. Commun.* **2003**, *311* (2), 329–336.
- (20) Martin, A. L.; Steurer, M. A.; Aronstam, R. S. Constitutive Activity among Orphan Class-A G Protein Coupled Receptors. *PLoS One* **2015**, *10* (9), No. e0138463.
- (21) Doyle, J. P.; Dougherty, J. D.; Heiman, M.; Schmidt, E. F.; Stevens, T. R.; Ma, G.; Bupp, S.; Shrestha, P.; Shah, R. D.; Doughty, M. L.; Gong, S.; Greengard, P.; Heintz, N. Application of a translational profiling approach for the comparative analysis of CNS cell types. *Cell* **2008**, *135* (4), 749–762.
- (22) Lobo, M. K.; Cui, Y.; Ostlund, S. B.; Balleine, B. W.; Yang, X. W. Genetic control of instrumental conditioning by striatopallidal neuron-specific S1P receptor Gpr6. *Nat. Neurosci.* **2007**, *10* (11), 1395–1397.
- (23) Oeckl, P.; Hengerer, B.; Ferger, B. G-protein coupled receptor 6 deficiency alters striatal dopamine and cAMP concentrations and reduces dyskinesia in a mouse model of Parkinson's disease. *Exp. Neurol.* **2014**, *257*, 1–9.
- (24) Beaulieu, J. M.; Espinoza, S.; Gainetdinov, R. R. Dopamine receptors - IUPHAR Review 13. *Br. J. Pharmacol.* **2015**, *172* (1), 1–23.
- (25) Perez, X. A.; Zhang, D.; Bordia, T.; Quik, M. Striatal D1 medium spiny neuron activation induces dyskinesias in parkinsonian mice. *Mov. Disord.* **2017**, *32* (4), 538–548.
- (26) Cenci, M. A. Presynaptic Mechanisms of L-DOPA-Induced Dyskinesia: The Findings, the Debate, and the Therapeutic Implications. *Front Neurol* **2014**, *5*, 242.
- (27) Dahlin, J. L.; Nissink, J. W.; Strasser, J. M.; Francis, S.; Higgins, L.; Zhou, H.; Zhang, Z.; Walters, M. A. PAINS in the assay: chemical mechanisms of assay interference and promiscuous enzymatic inhibition observed during a sulfhydryl-scavenging HTS. *J. Med. Chem.* **2015**, *58* (5), 2091–2113.
- (28) Riley, R. J.; Grime, K.; Weaver, R. Time-dependent CYP inhibition. *Expert Opin. Drug Metab. Toxicol.* **2007**, *3* (1), 51–66.
- (29) Macdonald, T. L.; Zirvi, K.; Burka, L. T.; Peyman, P.; Guengerich, F. P. Mechanism of cytochrome P450 inhibition by cyclopropylamines. *J. Am. Chem. Soc.* **1982**, *104*, 2050–2052.
- (30) Alavi, M. S.; Shamsizadeh, A.; Azhdari-Zarmehri, H.; Roohbakhsh, A. Orphan G protein-coupled receptors: The role in CNS disorders. *Biomed. Pharmacother.* **2018**, *98*, 222–232.
- (31) Morales, P.; Isawi, I.; Reggio, P. H. Towards a better understanding of the cannabinoid-related orphan receptors GPR3, GPR6, and GPR12. *Drug Metab. Rev.* **2018**, *50* (1), 74–93.
- (32) Song, Z. H.; Modi, W.; Bonner, T. I. Molecular cloning and chromosomal localization of human genes encoding three closely related G protein-coupled receptors. *Genomics* **1995**, *28* (2), 347–349.
- (33) Lovering, F.; Bikker, J.; Humblet, C. Escape from flatland: increasing saturation as an approach to improving clinical success. *J. Med. Chem.* **2009**, *52* (21), 6752–6756.
- (34) Lovering, F. Escape from Flatland 2: complexity and promiscuity. *MedChemComm* **2013**, *4* (3), 515.
- (35) Pedregal, C.; Joshi, E. M.; Toledo, M. A.; Lafuente, C.; Diaz, N.; Martinez-Grau, M. A.; Jimenez, A.; Benito, A.; Navarro, A.; Chen, Z.; Mudra, D. R.; Kahl, S. D.; Rash, K. S.; Statnick, M. A.; Barth, V. N. Development of LC-MS/MS-based receptor occupancy tracers and positron emission tomography radioligands for the nociceptin/orphanin FQ (NOP) receptor. *J. Med. Chem.* **2012**, *55* (11), 4955–4967.
- (36) Jesudason, C. D.; DuBois, S.; Johnson, M.; Barth, V. N.; Need, A. B., et al. In Vivo Receptor Occupancy in Rodents by LC-MS/MS. <https://www.ncbi.nlm.nih.gov/books/NBK424998/>.
- (37) Kin, K.; Yasuhara, T.; Kameda, M.; Date, I. Animal Models for Parkinson's Disease Research: Trends in the 2000s. *Int. J. Mol. Sci.* **2019**, *20* (21), 5402.
- (38) Brice, N. L.; Schiffer, H. H.; Monenschein, H.; Mulligan, V. J.; Page, K.; Powell, J.; Xu, X.; Cheung, T.; Burley, J. R.; Sun, H.; Dickson, L.; Murphy, S. T.; Kaushal, N.; Sheardown, S.; Lawrence, J.; Chen, Y.; Bartkowski, D.; Kanta, A.; Russo, J.; Hosea, N.; Dawson, L. A.; Hitchcock, S. H.; Carlton, M. B. Development of CVN₄₂₄: a selective and novel GPR6 inverse agonist effective in models of Parkinson's Disease. *J. Pharmacol. Exp. Ther.* **2021**, DOI: 10.1124/jpet.120.000438.